Electronic Supplementary Information for

Neutral Redox-active Hydrogen- and Halogen-Bonding [2]Rotaxanes for the Electrochemical Sensing of Chloride

Jason Y.C. Lim[a] , Matthew J. Cunningham[b], Jason J. Davis[b] and Paul D. Beer*[a]

[a] Chemistry Research Laboratory, Department of Chemistry, University of Oxford, Mansfield Road, Oxford, OX1 3TA, UK.
[b] Physical & Theoretical Chemistry Laboratory, South Parks Road, Oxford, OX1 3TA (UK).

E-mail: paul.beer@chem.ox.ac.uk

Contents

1. Synthesis of Ferrocene-appended macrocycles 7a-d

Tert-butyl macrocycle **7a**

To a suspension of 5-*tert*-butyl isophthalic acid (65.2 mg, 0.293 mmol) in dry CH_2Cl_2 (5.0 mL) was added oxalyl chloride (0.075 mL, 0.880 mmol), along with catalytic quantities of *N,N* – dimethylformamide. The mixture was stirred under N_2 for 3 hours to obtain a clear solution. Removal of solvent *in vacuo* gave the corresponding bis-acid chloride as a yellow solid, which was then re-dissolved in dry CH_2Cl_2 (8.0 mL) and taken up in a syringe. Separately, **6** (207 mg, 0.293 mmol) was dissolved in dry CH_2Cl_2 (8.0 mL) and taken up in a syringe. The contents of both syringes were added to a vigorously stirred solution of dry triethylamine (0.25 mL, 1.76 mmol) in dry CH_2Cl_2 (400 mL) over 4 hours using a syringe pump, and the resulting solution was stirred overnight under N_2. The clear orange reaction mixture was concentrated till a volume of c.a. 50 mL before being washed with 1M HCl (20 mL), followed by water (2 x 20 mL). Following drying with $MgSO_4$, the solvent was removed to yield a red-brown solid which was purified with silica gel chromatography (2 % CH_3OH in CH_2Cl_2) to give macrocycle **7a** as an orange solid (58 mg, 22 %). **^{1}H-NMR** (400 MHz, 1:1 $CDCl_3$/ CD_3OD) δ 8.08 (2H, s, Ar*H* ferrocene isophthalate), 8.04 (2H, s, Ar*H* *tert*-butyl isophthalate), 8.00 (2H, m, Ar*H* ferrocene and *tert*-butyl isophthalates), 6.79 (8H, s, Ar*H* hydroquinone), 4.73 (2H, s, Fc*H*), 4.34 (2H, s, Fc*H*), 4.05 - 4.10 (8H, m, CH_2O), 3.98 (5H, s, Fc*H*), 3.76 – 3.80 (8H, m, CH_2NH$_2$), 1.33 (9H, s, *tert*-butyl-*H*); **^{13}C-NMR** (100 MHz, 1:1 $CDCl_3$/ CD_3OD) δ 168.4, 168.1, 153.0, 152.5, 141.4, 134.3, 133.9, 127.9, 127.8, 122.2, 122.1, 155.4, 83.0, 69.5, 67.1, 66.5, 39.7, 39.7 (repeat), 34.9, 30.7 ; **MS** (ESI +ve) *m/z* 915.3034 ([M + Na]$^+$, $C_{50}H_{52}FeN_4NaO_8$, calc. 915.3028).

Bis-ferrocene-appended macrocycle **7b**

5-ferrocene isophthalic acid **3** (99.1 mg, 0.283 mmol) was suspended in dry CH_2Cl_2 (5.0 mL) containing catalytic quantities of *N,N* – dimethylformamide and cooled to 0 ^{o}C . Oxalyl chloride (0.073 mL, 0.849 mmol) was added dropwise and the reaction was stirred for 2 h under N_2 till a clear red solution was obtained. The solvent was then removed *in vacuo* to yield the bis-acid chloride as a red-brown solid, which was then redissolved in dry CH_2Cl_2 (6 mL) and loaded into a syringe. **6** (200 mg, 0.283 mmol) was dissolved in dry CH_2Cl_2 (6.0 mL) containing triethylamine (0.24 mL, 1.70 mmol) and loaded into another syringe. The contents of both syringes were added to vigorously-stirred dry CH_2Cl_2 (450 mL) dropwise using a syringe pump over 3 h, and stirred overnight under N_2. The reaction mixture was then concentrated to approximately 50 mL, and washed with 10 % HCl (20 mL), followed by water (3 x 20 mL). The combined organics were dried with $MgSO_4$ and dried *in vacuo* to give an orange-brown solid. Purification via silica gel chromatography (3 % CH_3OH in CH_2Cl_2) yielded **7b** as an orange solid (57.9 mg, 20 %). **^{1}H-NMR** (400 MHz, 1:1 $CDCl_3$/ CD_3OD) δ 8.10 (4H, s, Ar*H*), 7.98 (2H, s, Ar*H*), 6.83 (s, 8H, hydroquinone-*H*), 4.77 (4H, s, Fc*H*), 4.36 (4H, s, Fc*H*), 4.09 (8H, t, ^3J = 4.7 Hz, CH_2O), 4.00 (10H, s, Fc*H*), 3.80 (8H, t, ^3J = 5.0 Hz, CH_2NH); **^{13}C-NMR** (100 MHz, 1:1 $CDCl_3$/ CD_3OD) δ 167.6, 152.7, 141.2, 134.1, 127.7, 121.5, 115.2, 82.7, 69.4, 66.9, 66.4, 49.0, 39.5; **MS** (ESI +ve) *m/z* 1043.2380 ([M + Na]$^+$, $C_{56}H_{52}Fe_2N_4NaO_8$, calc. 1043.2379).

Pyridine macrocycle **7c**

3,5-pyridine dicarboxylic acid (28.0 mg, 0.167 mmol) was suspended in dry CH_2Cl_2 (2.0 mL) at 0 ^oC . To this white suspension was added a drop of dry *N,N* – dimethylformamide followed by oxalyl chloride dropwise (0.043 mL, 0.501 mmol), and the reaction was allowed to stir for 2 hours under N_2 until a clear pale yellow solution was obtained. After removing the solvent *in vacuo*, the resulting off-white solid was redissolved in 6.0 mL of dry CH_2Cl_2 and taken up in a syringe. Separately, the ferrocene-functionalised bisamine macrocycle precursor **6** (117 mg, 0.164 mmol) and anhydrous triethylamine (0.14 mL, 1.00 mmol) was dissolved in 6.0 mL of dry CH_2Cl_2, and the resulting red solution was taken up in a syringe. The contents of both syringes were added dropwise over 4 hours to vigorously-stirred dry CH_2Cl_2 (300 mL) and the reaction was allowed to proceed overnight under N_2. Following which, the crude reaction mixture was concentrated till approximately 50 mL and washed with 10 % citric acid (2 x 30 mL) then water (2 x 30 mL). The organic layer was dried with $MgSO_4$ and the solvent removed *in vacuo* to obtain an orange solid. Silica gel column chromatography (5 % CH_3OH in CH_2Cl_2) yielded the macrocycle **7c** as an orange powder (34.0 mg, 25 %). **^{1}H-NMR** (400 MHz, d^6-DMSO) δ 9.09 (2H, s, Ar*H* pyridine isophthalamide), 8.98 (2H, t, ^3J = 4.0 Hz, CON*H* pyridine isophthalamide), 8.79 (2H, t, ^3J = 4.0 Hz, CON*H* ferrocene isophthalamide), 8.58 (1H, s, Ar*H* pyridine isophthalamide), 8.11 (1H, s, Ar*H* ferrocene isophthalamide), 8.09 (2H, s, Ar*H* ferrocene isophthalamide), 6.88 (8H, m, Ar*H* hydroquinone), 4.91 (2H, s, Fc*H*), 4.44 (2H, s, Fc*H*), 4.06 (8H, t, ^3J = 6.4 Hz, CH_2O), 4.04 (5H, s, Fc*H*), 3.63 (8H, m, CH_2NHCO) ; **^{13}C-NMR** (125 MHz, d^6-DMSO) δ 166.7, 165.2, 153.1, 153.0, 152.8, 151.0, 140.3, 135.2, 134.3, 130.0, 127.2, 124.2, 115.9, 83.8, 70.0, 69.9, 67.7, 67.1, 67.0, 50.1; **MS** (ESI +ve) 860.2339 *m/z* ([M + Na]$^+$, $C_{45}H_{43}FeN_5NaO_8$, calc. 860.2354).

Nitro-appended macrocycle **7d**

5-nitroisophthalic acid (35.0 mg, 0.167 mmol) and a drop of dry *N,N* – dimethylformamide was mixed with dry CH_2Cl_2 (2.0 mL) to give a white suspension which was then cooled to 0 ^oC, before oxalyl chloride (0.043 mL, 0.50 mmol) was added dropwise. After stirring for 2 hours, the clear yellow solution was dried *in vacuo* to afford the bis-acid chloride as a pale yellow solid. This was dissolved in 6.0 mL of dry CH_2Cl_2 and taken up in a syringe, and was added to vigorously-stirred dry CH_2Cl_2 (400 mL), together with the contents of another syringe containing **6** (116 mg, 0.164 mmol) and anhydrous triethylamine (0.14 mL, 1.0 mmol) dissolved in dry dichloromethane (6.0 mL), over a period of 3 hours using a syringe pump. The reaction was allowed to proceed overnight under N_2, before being concentrated *in vacuo* to a volume of 50 mL. After washing with 10 % citric acid (2 x 30 mL) and water (2 x 30 mL), the organic layer was dried over $MgSO_4$ and solvent removed to afford an orange solid. Silica gel column chromatography using 2 % CH_3OH in CH_2Cl_2 as eluent gave the macrocycle **7d** as an orange powder (54 mg, 37 %). **^{1}H-NMR** (400 MHz, d^6-DMSO) δ 9.17 (2H, t, ^3J = 5.0 Hz, NO_2ArCON*H*), 8.79 (2H, t, ^3J = 5.0 Hz, FcArCON*H*), 8.77 (2H, s, NO_2-Ar*H*), 8.74 (1H, s, NO_2-Ar*H*), 8.10 (1H, s, Fc-Ar*H*), 8.08 (2H, s, Fc-Ar*H*), 6.87 (8H, m, hydroquinone-Ar*H*), 4.90 (2H, s, Fc*H*), 4.43 (2H, s, Fc*H*), 4.07 (8H, m, -CH_2O), 4.03 (5H, s, Fc*H*), 3.64 (8H, m, -CH_2NHCO); **^{13}C-NMR** (125 MHz, d^6-DMSO) δ 166.6, 164.6, 153.2, 153.0, 148.4, 140.3, 136.5, 135.2, 132.6, 127.2, 124.8, 124.2,

116.0, 115.9, 83.8, 69.9, 69.9 (repeat), 67.1, 67.0, 66.8; **MS** (ESI +ve) *m/z* 904.2221 ($[M + Na]^+$, $C_{46}H_{43}FeN_5NaO_{10}$, calc. 904.2253).

S2. Spectral Characterisation of [2]Rotaxanes 1a-e

[2]Rotaxane **1a**

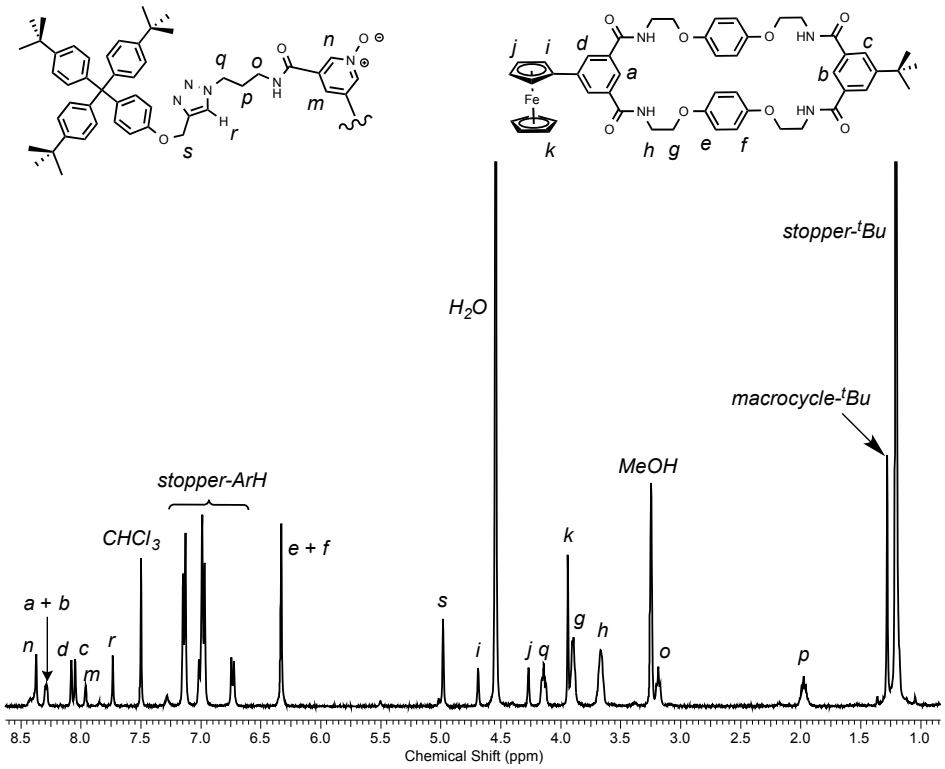

Fig S2-1. ^{1}H NMR of [2]rotaxane **1a** in 1:1 $CDCl_3$/ CD_3OD at 298 K (500 MHz).

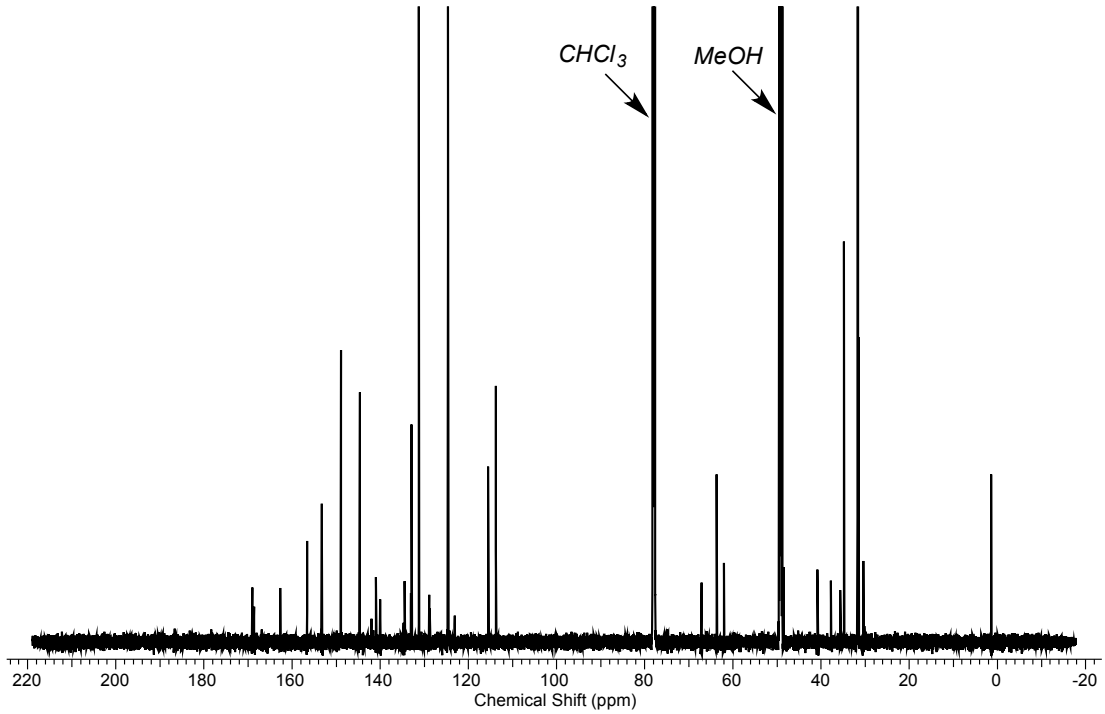

Fig S2-2. ^{13}C NMR of [2]rotaxane **1a** in 1:1 $CDCl_3$/ CD_3OD at 298 K (125 MHz).

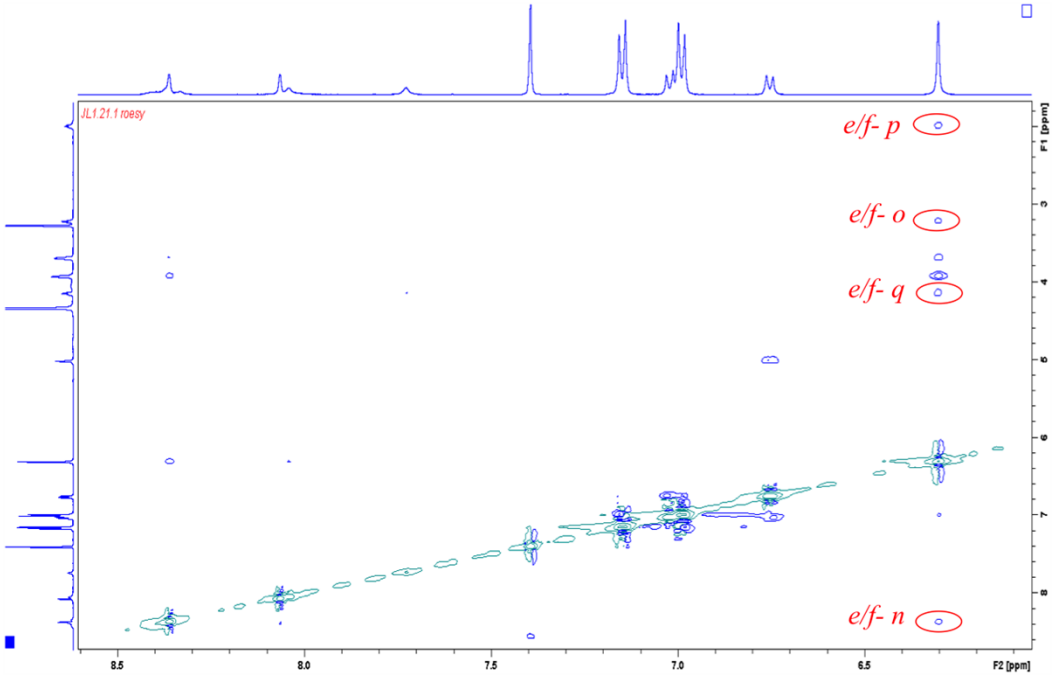

Fig. S2-3. ^{1}H ROESY spectrum of rotaxane **1a** in 1:1 $CDCl_3$/ CD_3OD at 298 K (500 MHz). Cross peaks indicative of the interlocked nature of the rotaxane are circled in red and proton labels follow those in **Fig. S2-1.**

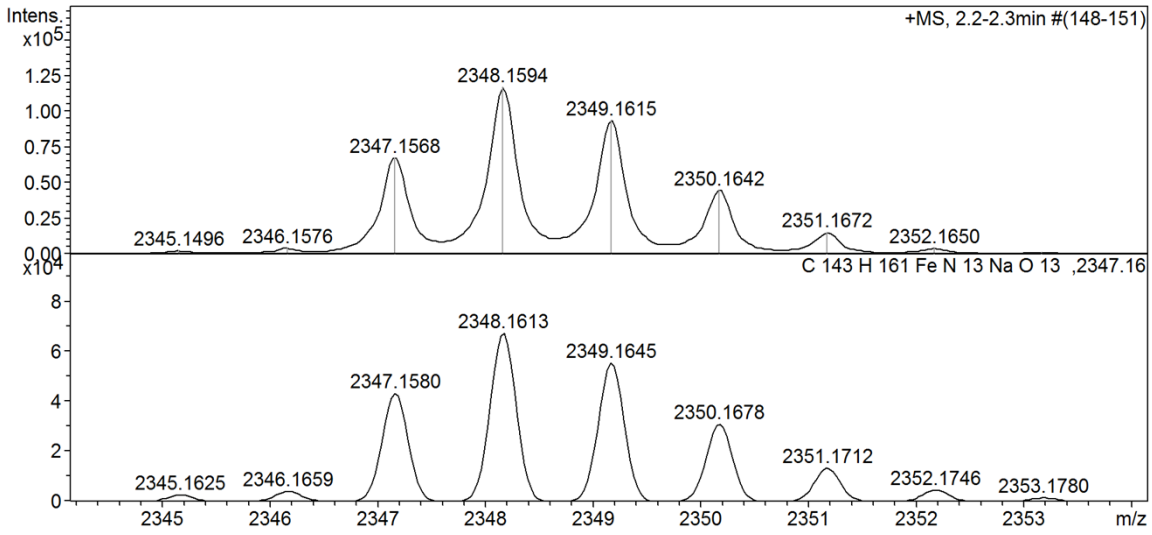

Fig. S2-4. High-resolution mass spectrum of rotaxane **1a**. **Top:** theoretical isotope model; **Bottom:** measured spectrum.

[2]Rotaxane **1b**

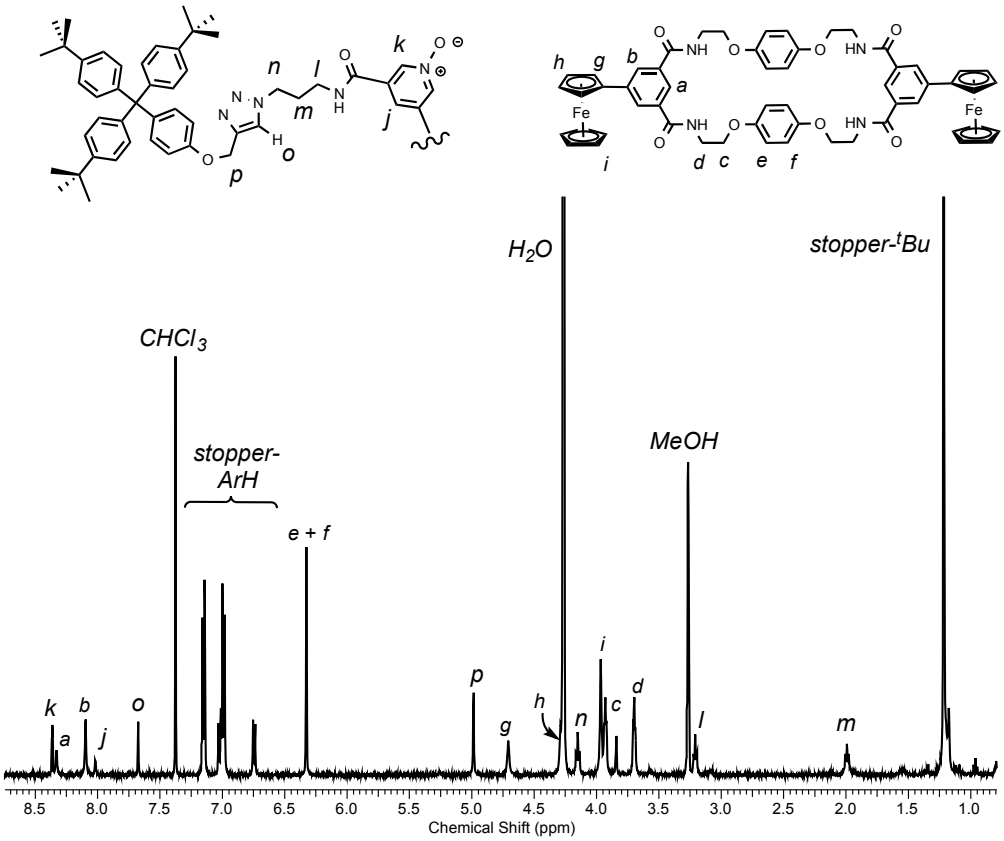

Fig S2-5. ^{1}H NMR of [2]rotaxane **1b** in 1:1 $CDCl_3$/ CD_3OD at 298 K (500 MHz).

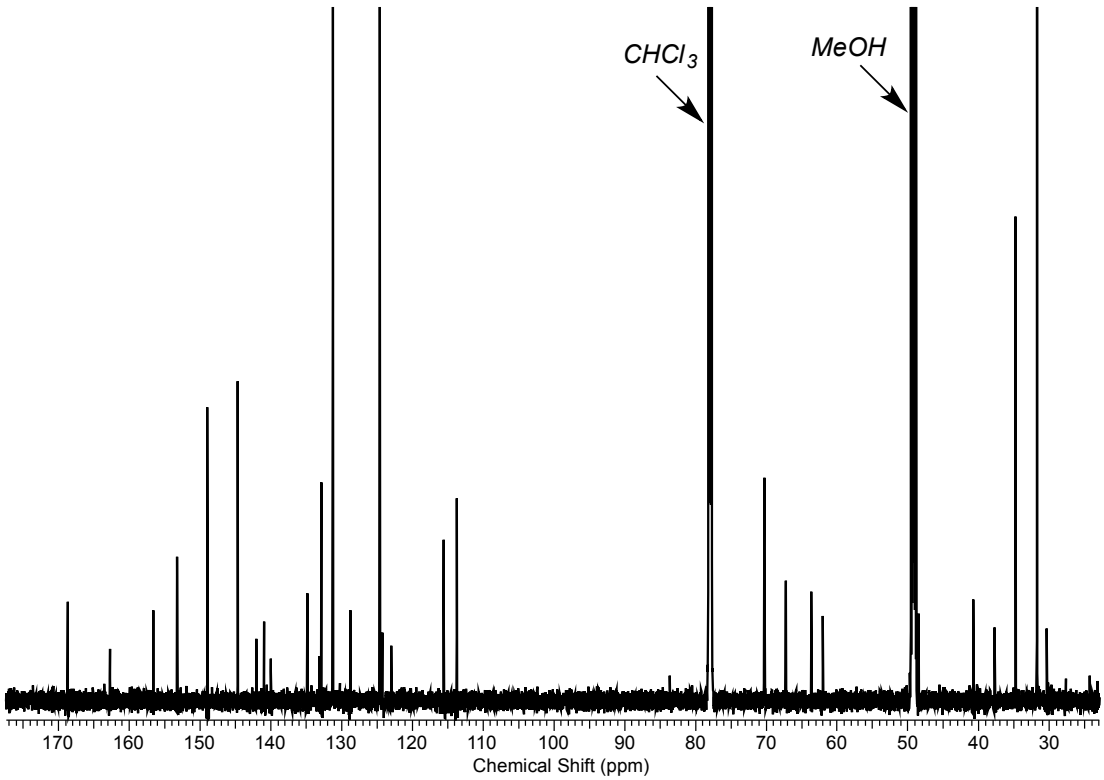

Fig S2-6. ^{13}C NMR of [2]rotaxane **1b** in 1:1 $CDCl_3$/ CD_3OD at 298 K (125 MHz).

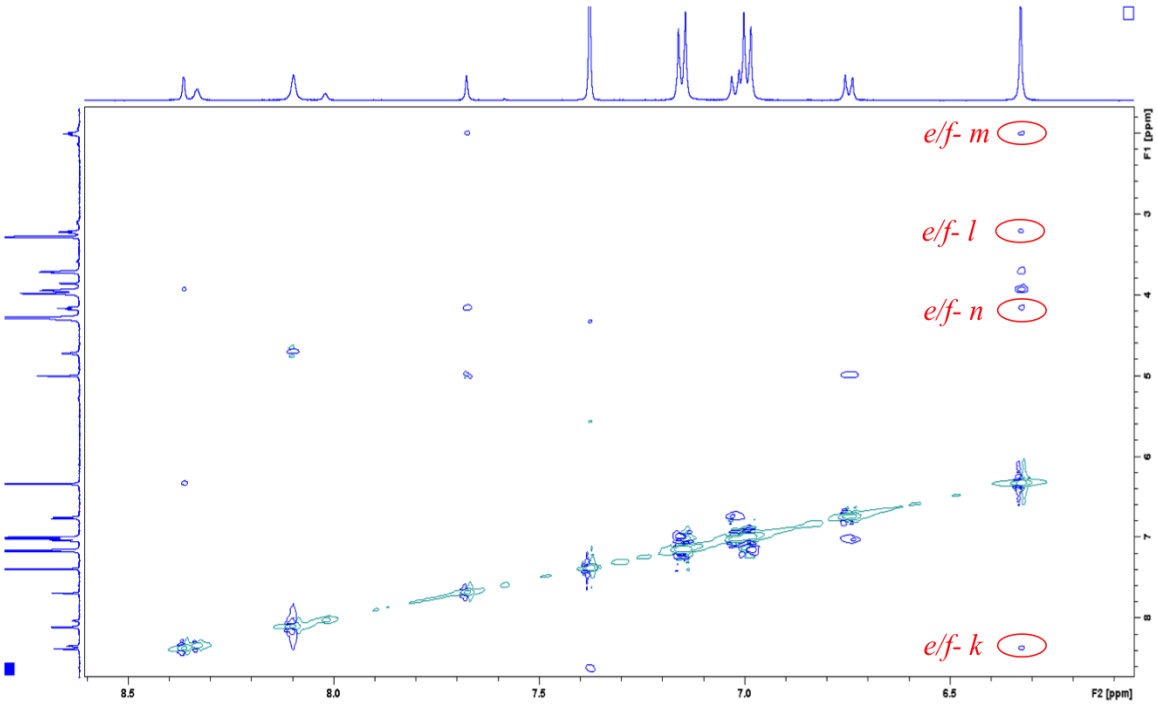

Fig. S2-7. ^{1}H ROESY spectrum of rotaxane **1b** in 1:1 $CDCl_3$/ CD_3OD at 298 K (500 MHz). Cross peaks indicative of the interlocked nature of the rotaxane are circled in red and proton labels follow those in **Fig. S2-5.**

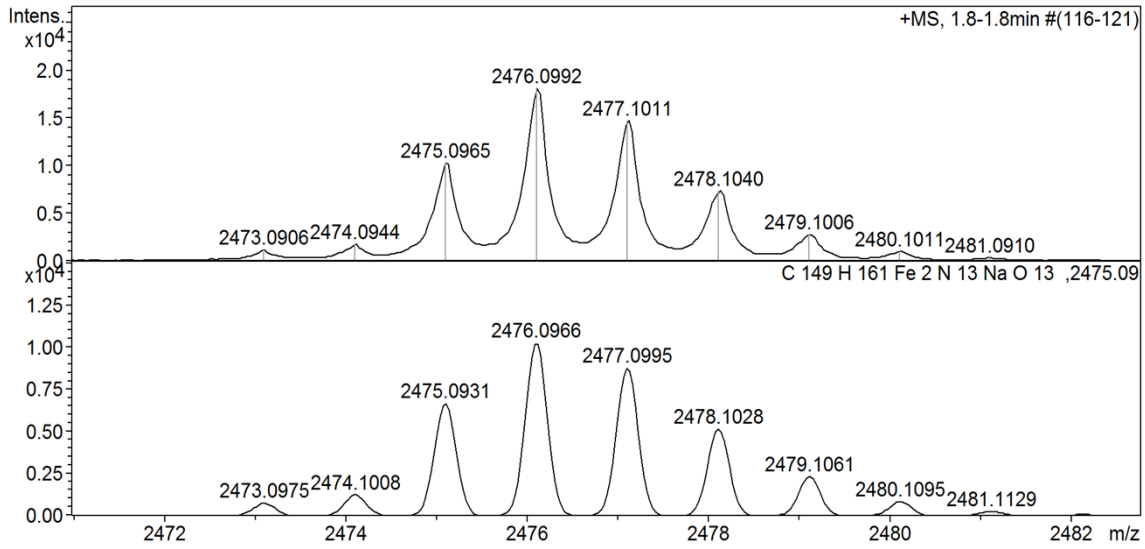

Fig. S2-8. High-resolution mass spectrum of rotaxane **1b**. **Top:** theoretical isotope model; **Bottom:** measured spectrum.

[2]Rotaxane **1c**

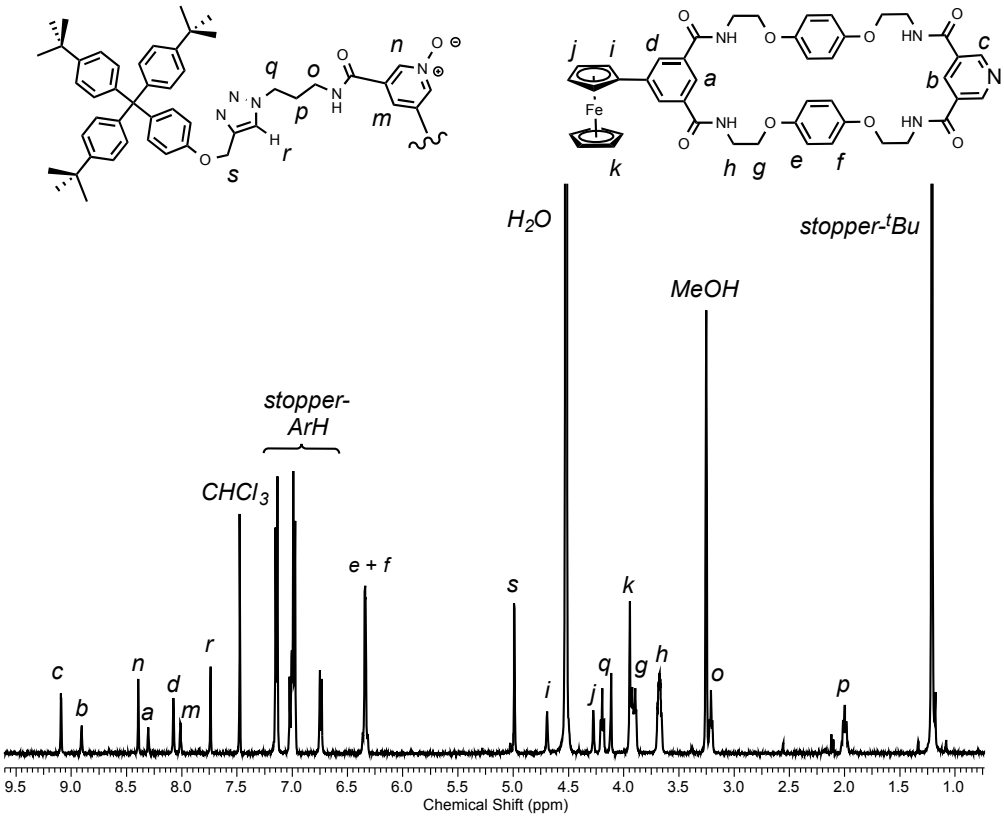

Fig S2-9. ^{1}H NMR of [2]rotaxane **1c** in 1:1 $CDCl_3$/ CD_3OD at 298 K (500 MHz).

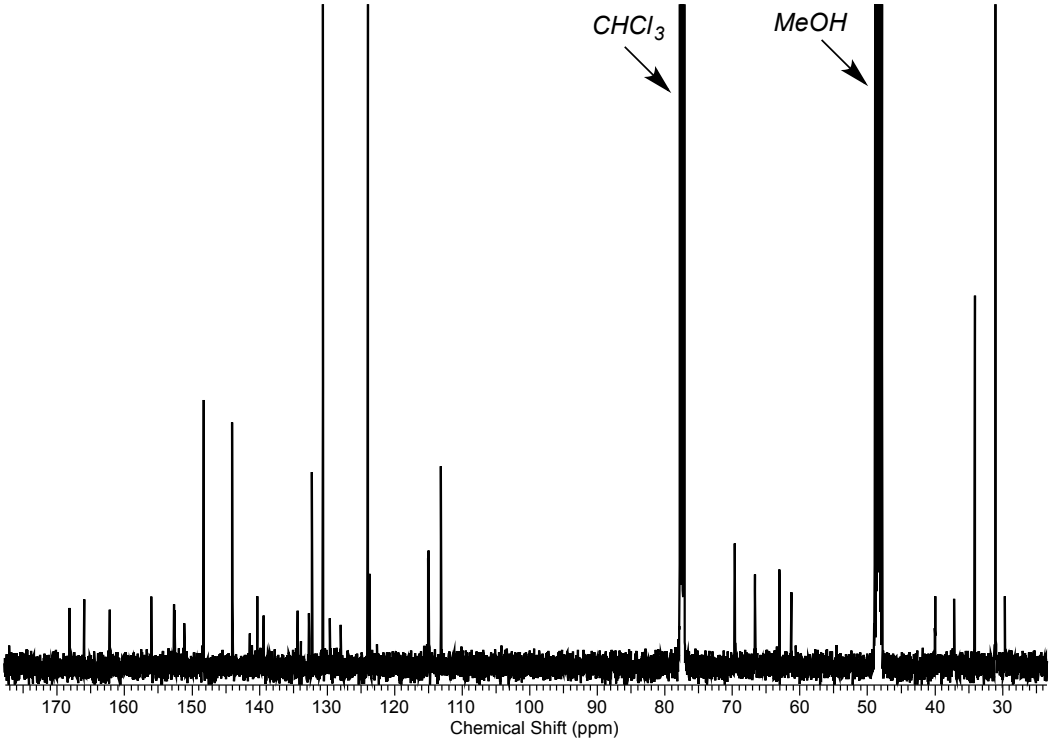

Fig S2-10. ^{13}C NMR of [2]rotaxane **1c** in 1:1 $CDCl_3$/ CD_3OD at 298 K (125 MHz).

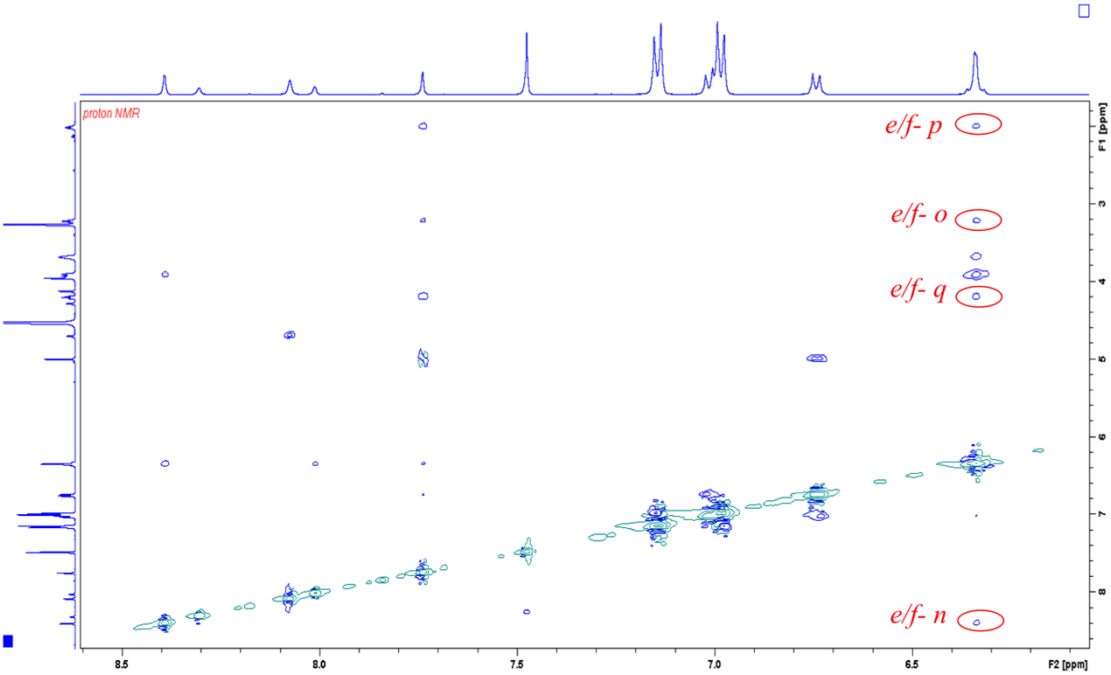

Fig. S2-11. ^{1}H ROESY spectrum of rotaxane **1c** in 1:1 $CDCl_3$/ CD_3OD at 298 K (500 MHz). Cross peaks indicative of the interlocked nature of the rotaxane are circled in red and proton labels follow those in **Fig. S2-9.**

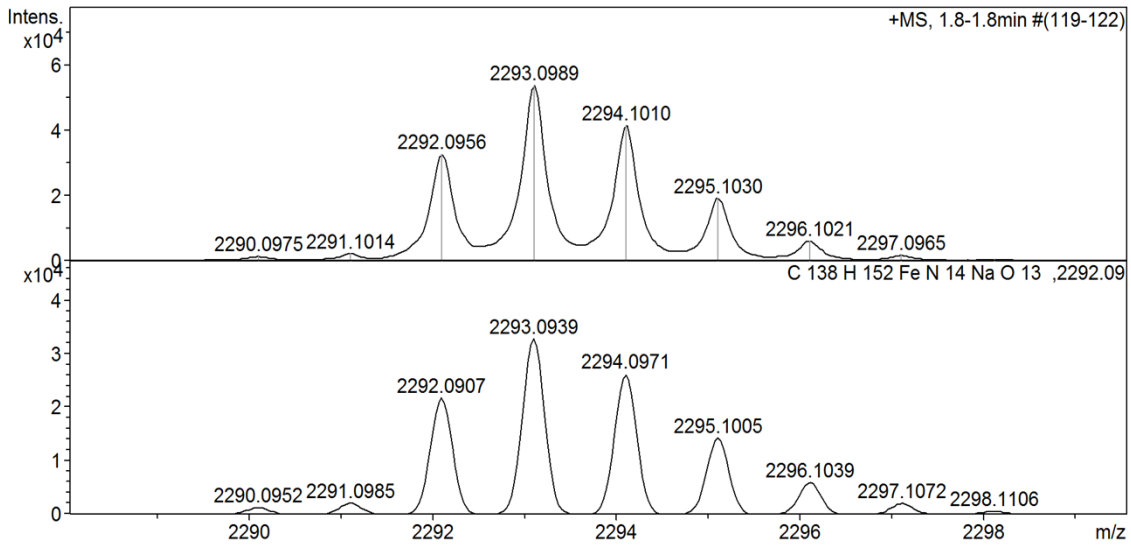

Fig. S2-12. High-resolution mass spectrum of rotaxane **1b**. **Top:** theoretical isotope model; **Bottom:** measured spectrum.

[2]Rotaxane **1d**

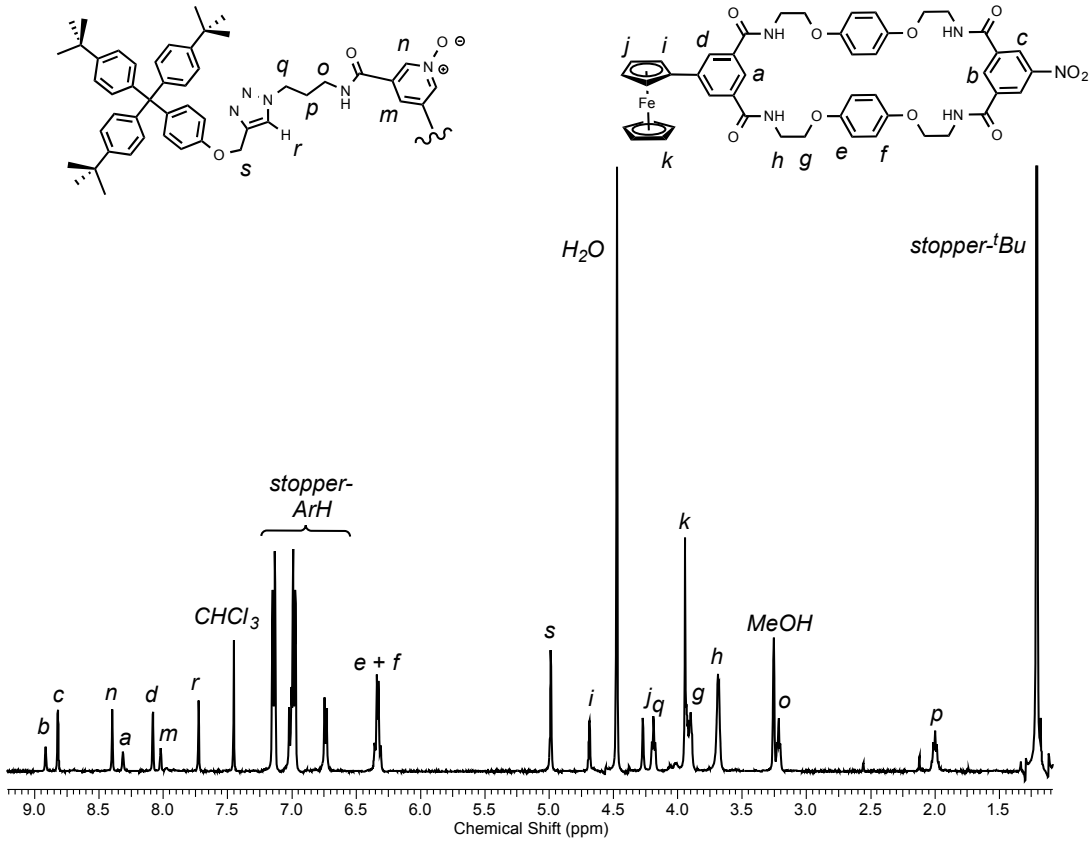

Fig S2-13. ^{1}H NMR of [2]rotaxane **1d** in 1:1 $CDCl_3$/ CD_3OD at 298 K (500 MHz).

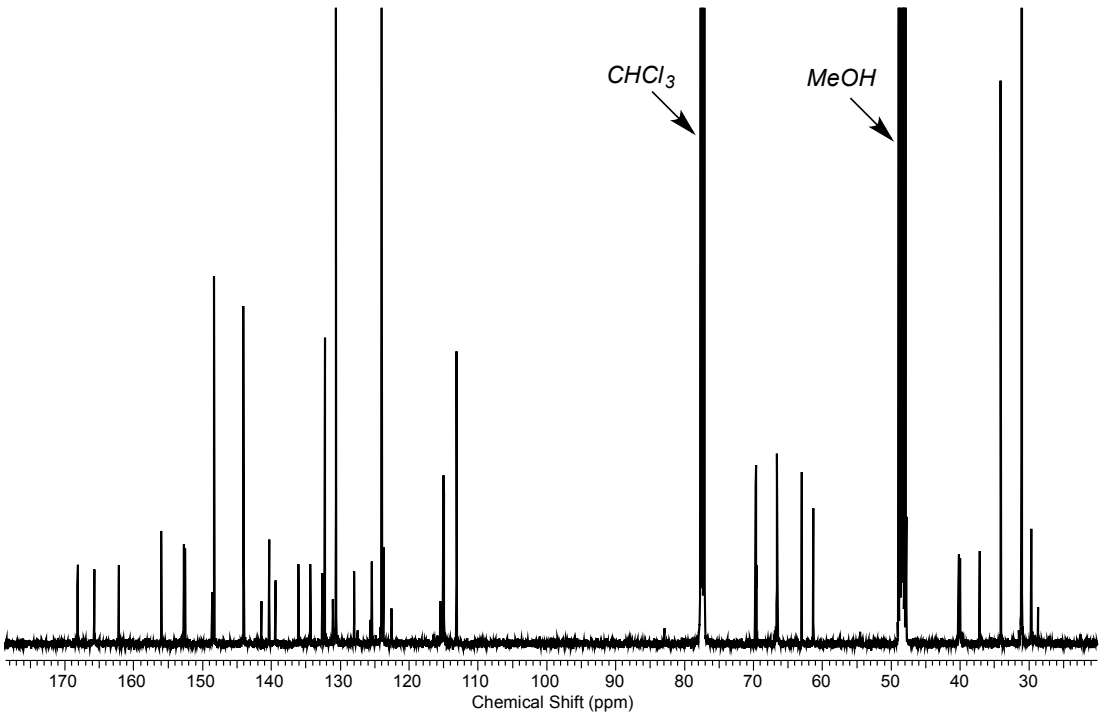

Fig S2-14. ^{13}C NMR of [2]rotaxane **1d** in 1:1 $CDCl_3$/ CD_3OD at 298 K (125 MHz).

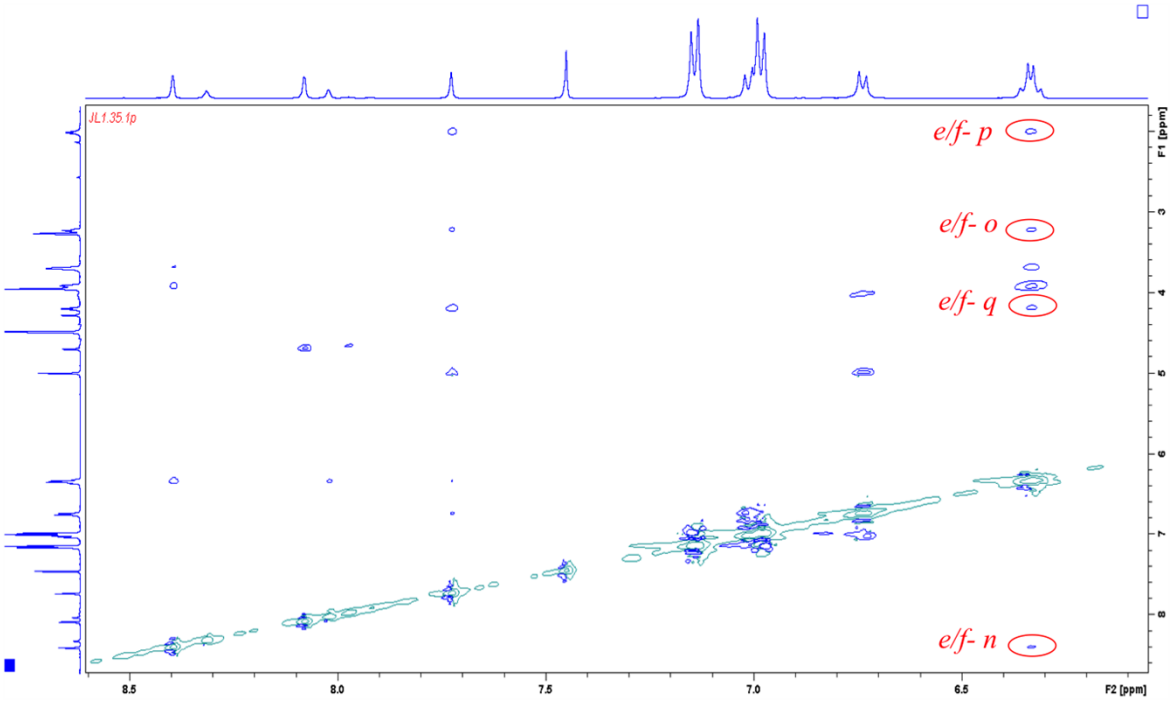

Fig. S2-15. ^{1}H ROESY spectrum of rotaxane **1d** in 1:1 $CDCl_3$/ CD_3OD at 298 K (500 MHz). Cross peaks indicative of the interlocked nature of the rotaxane are circled in red and proton labels follow those in **Fig. S2-13.**

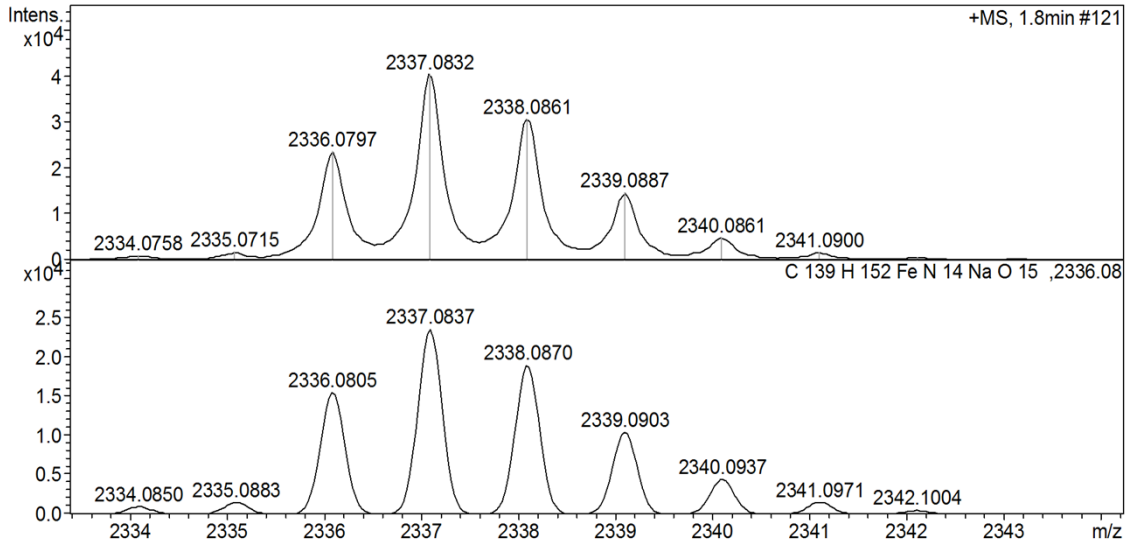

Fig. S2-16. High-resolution mass spectrum of rotaxane **1d**. **Top:** theoretical isotope model; **Bottom:** measured spectrum.

[2]Rotaxane **1e**

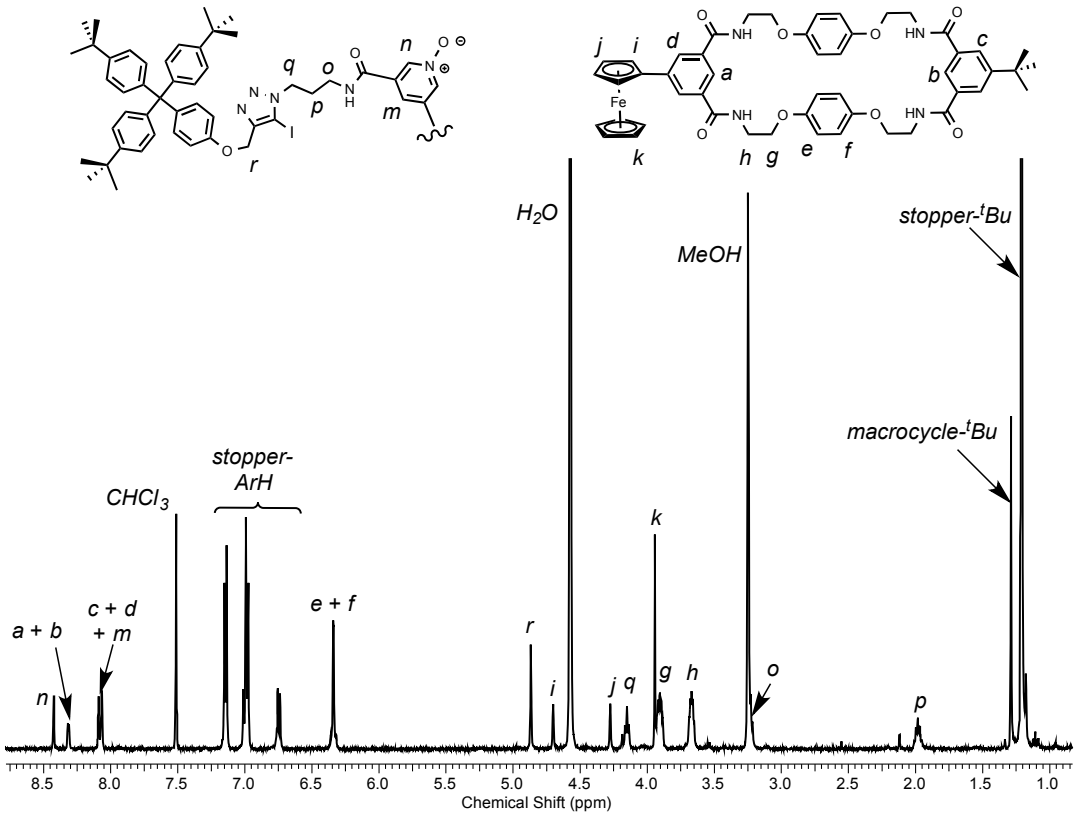

Fig S2-17. ^{1}H NMR of [2]rotaxane **1e** in 1:1 $CDCl_3$/ CD_3OD at 298 K (500 MHz).

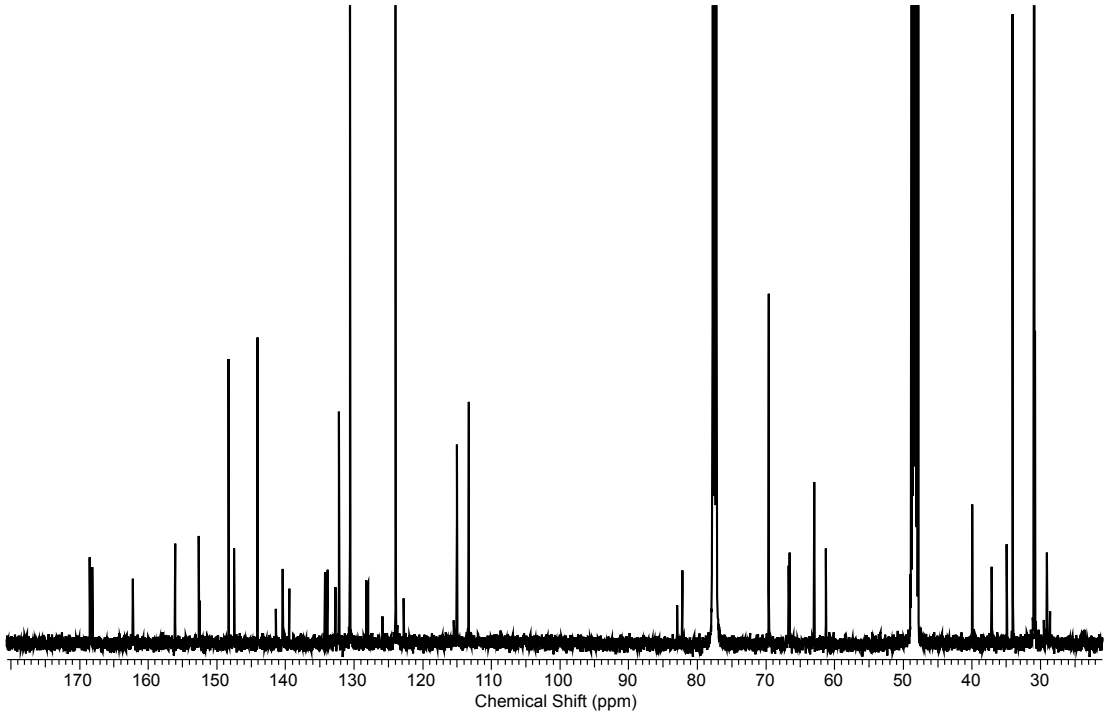

Fig S2-18. ^{13}C NMR of [2]rotaxane **1e** in 1:1 $CDCl_3$/ CD_3OD at 298 K (125 MHz).

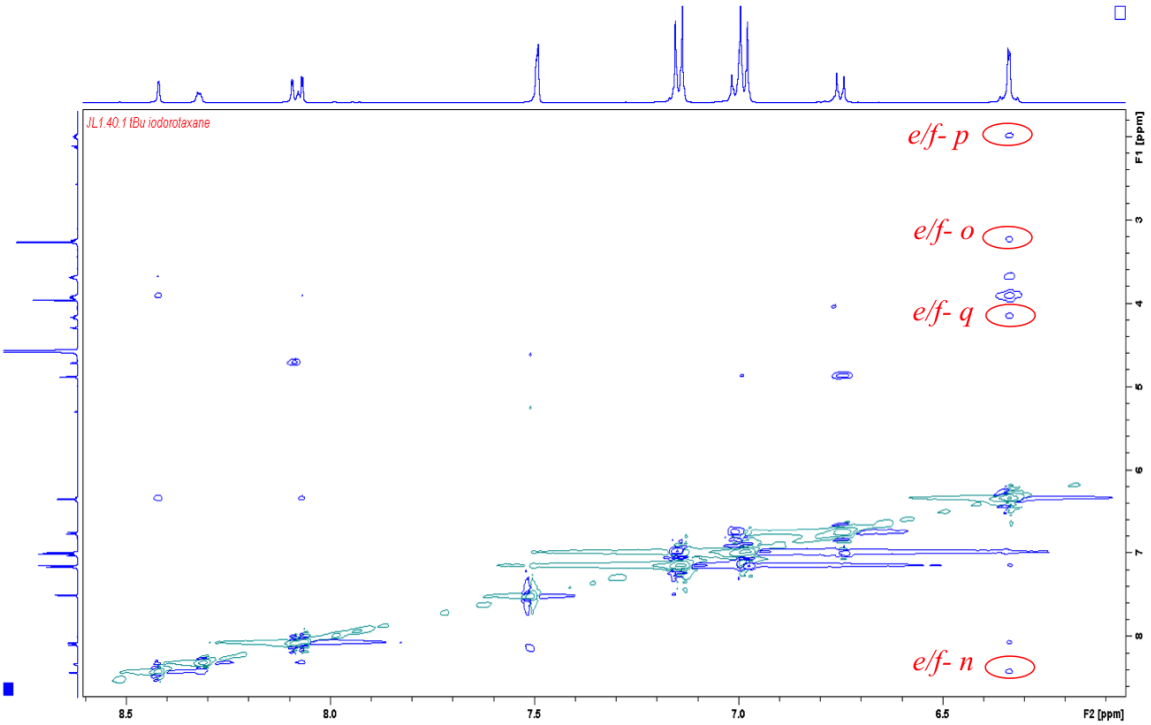

Fig. S2-19. ^{1}H ROESY spectrum of rotaxane **1e** in 1:1 $CDCl_3$/ CD_3OD at 298 K (500 MHz). Cross peaks indicative of the interlocked nature of the rotaxane are circled in red and proton labels follow those in **Fig. S2-17.**

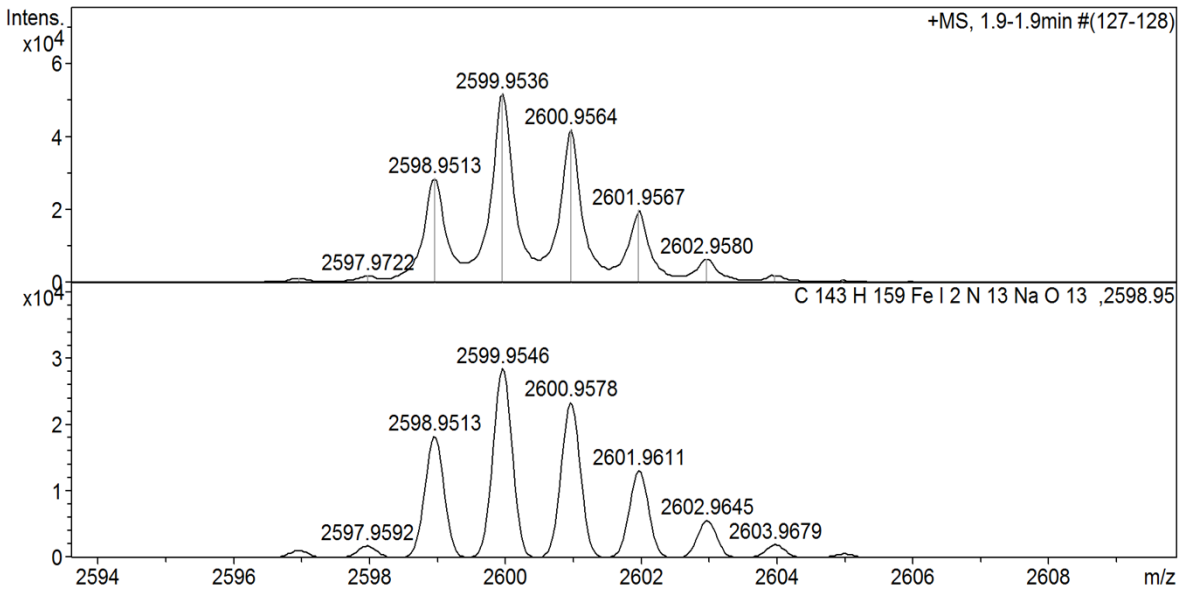

Fig. S2-20. High-resolution mass spectrum of rotaxane **1e**. **Top:** theoretical isotope model; **Bottom:** measured spectrum.

S3. Anion Recognition Studies of [2]Rotaxanes by ^{1}H NMR titrations

General Protocol

^{1}H NMR titration experiments were performed on a Bruker AVIII 500 MHz spectrometer. In a typical experiment, a solution of the appropriate tetrabutylammonium (TBA) salt was added to the [2]rotaxane solution at 298 K. Both TBA salt and rotaxane were dissolved in a solvent mixture containing $CDCl_3$/ CD_3OD/ D_2O in 45:45:10 ratio. TBA was chosen as the counter-cation due to its non-coordinating nature. A 0.075 M solution of the salt was added to 0.50 mL of a 1.5 mM solution of rotaxane, where 1.0 equivalent of salt added corresponds to 10 μL of the salt solution. The chemical shift of the internal isophthalamide protons, pyridine *N*–oxide proton and triazole proton for bis-prototriazole rotaxanes **1a-d** and the same protons except the triazole ones for bis-iodotriazole rotaxane **1e** were monitored for 17 data points corresponding to 0.0, 0.2, 0.4, 0.6, 0.8, 1.0, 1.2, 1.4, 1.6, 1.8, 2.0, 2.5, 3.0, 4.0, 5.0, 7.0 and 10.0 equivalents of added guest anion.

The binding of anions in the [2]rotaxanes **1a-e** were found to be fast on the NMR timescale. The values of the observed chemical shift and concentration of anion were entered into the WinEQNMR2[1] computer programme for every titration point. From initial estimates made of the binding constants and limiting chemical shifts, these parameters were refined using non-linear least-squares analyses to obtain the best fit between empirical and calculated chemical shifts based on a 1:1 binding stoichiometry. The input parameters were varied till convergence of the best fit values of the binding constants and their errors were obtained.

For [2]rotaxanes **1a-e**, all protons monitored gave nearly identical values of binding constants. Hence in all cases that follow, the pyridine *N*–oxide proton for each rotaxane will be used to represent the titration results. In Fig. S3.1 – S3.4, empirical data points are represented by the filled dots, while continuous lines represent the calculated binding curves.

^{1}H NMR titration data

Binding curves for [2]rotaxane **1a** are shown in the main article as **Fig. 4**. All titrations were carried out with the solvent mixture of $CDCl_3$/ CD_3OD/ D_2O 45:45:10 at 298 K.

[2]Rotaxane **1b**

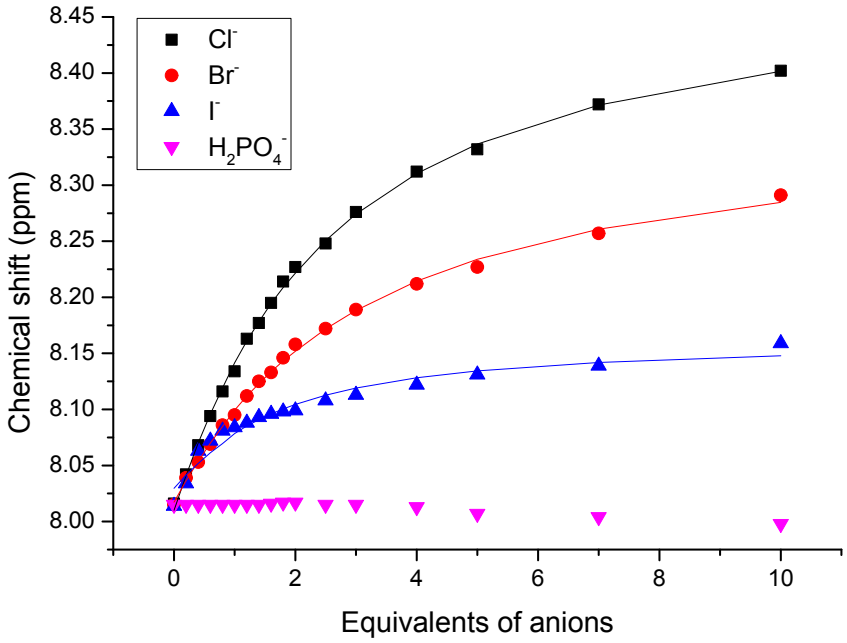

Fig. S3-1. Changes in chemical shift of the internal pyridine *N* – oxide proton upon addition of increasing quantities of TBA salt to the NMR solution of rotaxane **1b**.

[2]Rotaxane **1c**

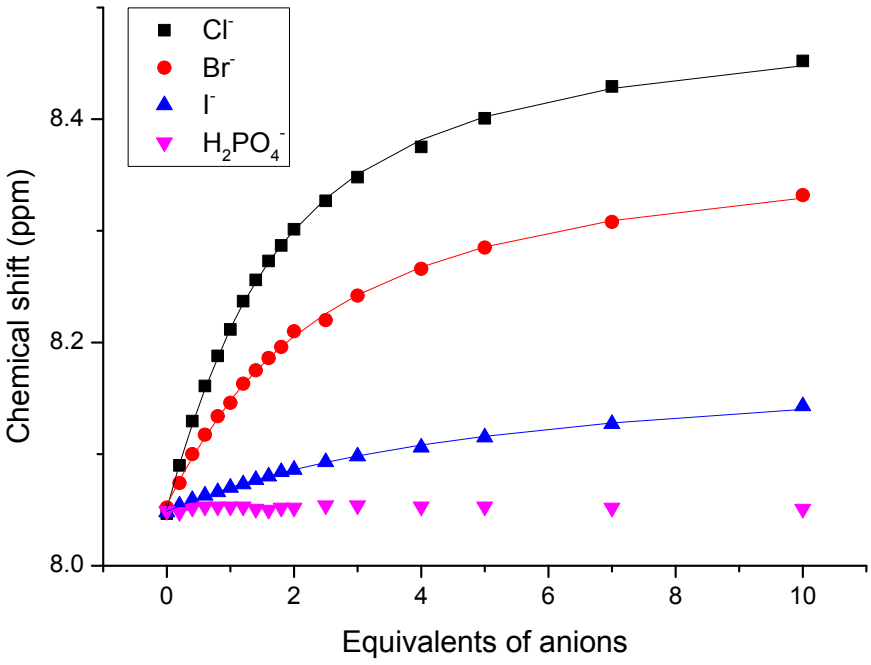

Fig. S3-2. Changes in chemical shift of the internal pyridine *N* – oxide proton on addition of increasing quantities of TBA salt to the NMR solution of rotaxane **1c**.

[2]Rotaxane **1d**

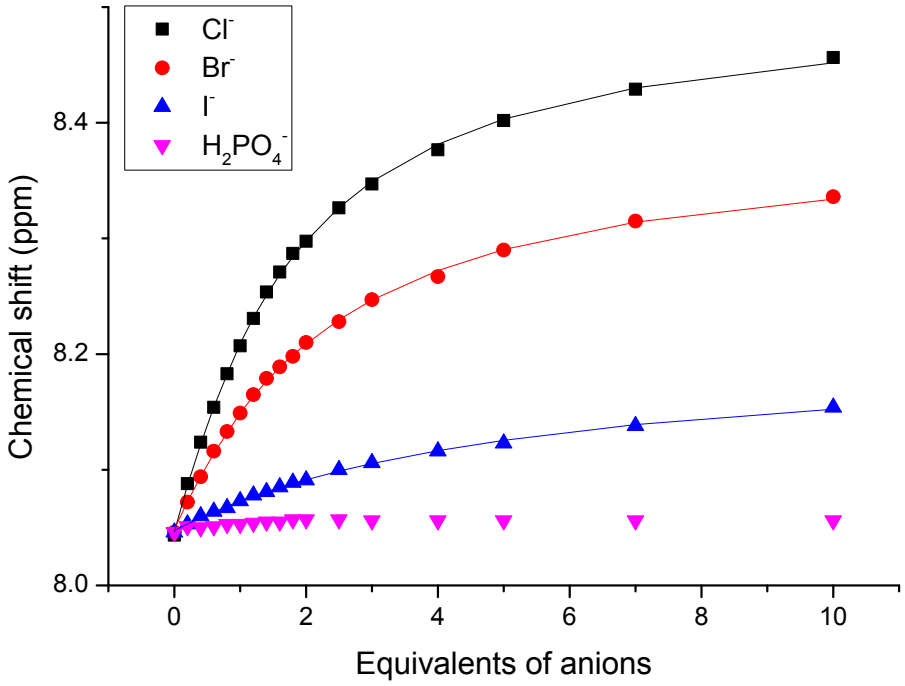

Fig. S3-3. Changes in chemical shift of the internal pyridine *N* – oxide proton on addition of increasing quantities of TBA salt to the NMR solution of rotaxane **1d**.

[2]Rotaxane **1e**

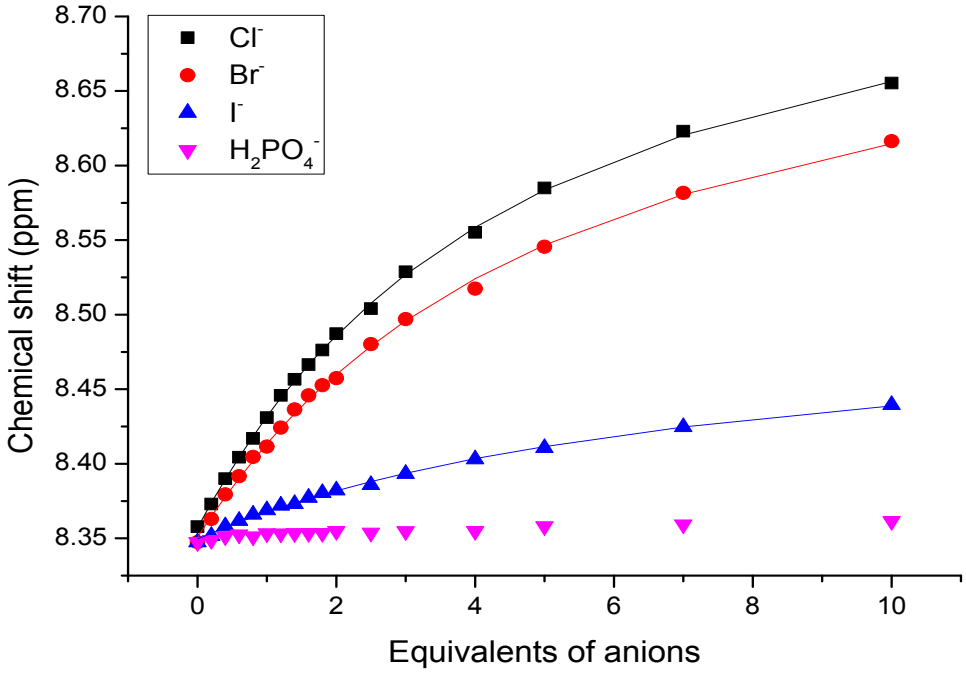

Fig. S3-4. Changes in chemical shift of the internal pyridine *N* – oxide proton on addition of increasing quantities of TBA salt to the NMR solution of bis-iodotriazole [2]rotaxane **1e**.

4. Electrochemical Studies

General Protocol

Cyclic voltammetry (CV) was performed on an Autolab PGSTAT-12 system and all data was analyzed using General Purpose Electrochemical Software (GPES) version 4.9. All electrochemistry was undertaken in anhydrous acetonitrile – dichloromethane (1:1), with 0.1 M $TBAPF_6$ supporting electrolyte. All diffusive voltammetry was undertaken at a 3 mm diameter glassy carbon working electrode (BASi), cleaned prior to use using 0.3 micron alumina powder (Buehler), and all potentials were referenced to a Ag / $AgNO_3$ reference electrode[2]; the latter was prepared using an anhydrous acetonitrile-based solution of 10 mM $AgNO_3$ and 0.15 M $TBAPF_6$. A Ag/$AgNO_3$ reference electrode was used in preference to the more commonly used Ag/AgCl reference electrode in order to prevent any potential interference in the sensory response of the rotaxanes arising from any chloride anion leakage. All solutions were degassed with dry nitrogen prior to the recording of each CV. CVs were recorded with a 1 s equilibration time, step potential of 1 mV and at a scan rate of 100 mV s^{-1}. For all the host systems investigated, the host was dissolved in the electrolyte solution to afford a concentration of 0.5 mM. The electrochemical reversibility of each system was probed by vitue of varying the scan rate (25, 50, 75, 100, 250, 500 mV s^{-1}). After which, electrochemical anion binding experiments were performed by adding known aliquots of anions, (as a 0.25 M solution in the same electrolyte mixture) corresponding to 0.0, 0.5, 1.0, 2.0 and 5.0 equivalents, respectively.

Prior to utilising the Ag / $AgNO_3$ working electrode, a ^1H NMR titration experiment was performed in the presence of $TBANO_3$ and [2]rotaxane **1b** (solutions prepared as described in Section S3). As shown in **Fig. S4-1**, the addition of 10.0 equivalents of $TBANO_3$ brought about NMR peak shifts of < 0.1 ppm, giving binding constants too small to be calculated using the WinEQNMR2 programme. Hence the nitrate anion does not bind in the cavity of the rotaxanes.

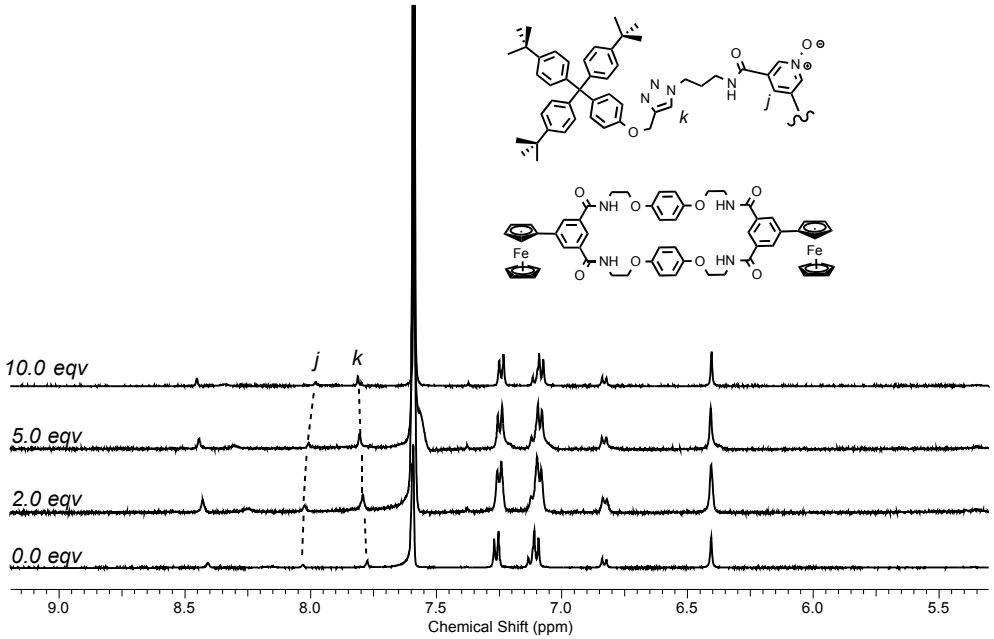

Fig S4-1. ^1H NMR spectra of titration experiments with [2]rotaxane **1b** and $TBANO_3$ in $CDCl_3$/ CD_3OD/ D_2O = 45:45:10 at 298 K (500 MHz).

Electrochemical Reversibility Studies

The electrochemical reversibility of our host systems are probed by recording CV scans at different scan rates. An electrochemical system is described as reversible, and hence exhibits fast electron transfer kinetics, when the following criteria are met:

1. ΔE_p = (59 / n) mV, where n = number of electrons transferred in the redox process. For our ferrocene-appended host systems, n = 1 during ferrocene redox chemistry. Hence, ΔE_p should be 59 mV for our systems.
2. Potentials E_{pa} and E_{pc} corresponding to peak oxidation and reduction currents respectively are independent of the scan rate.
3. The peak cathodic (I_{pc}) and anodic (I_{pa}) currents are of equal magnitude, i.e. $I_{pc} / I_{pa} = 1$.
4. The peak currents are proportional to the square root of the CV scan rate.

Unless otherwise stated, all CVs are recorded in 0.1 M $TBAPF_6$ electrolyte solution (CH_2Cl_2/ CH_3CN = 1:1) and potentials are compared to the Ag / $AgNO_3$ reference electrode.

Macrocycle **7a**

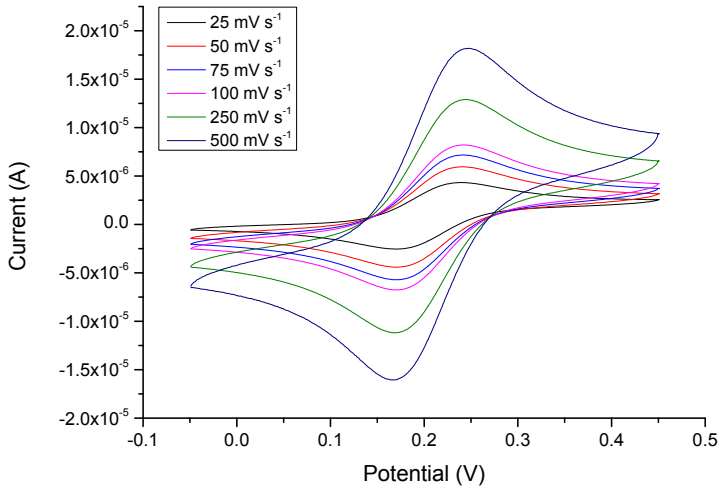

Fig. S4-2. CVs of macrocycle **7a** at different scan rates.

Table S4-1. Values of E_{pc}, E_{pa}, I_{pa}, I_{pc} ΔE_p and I_{pa}/ I_{pc} for macrocycle **7a** recorded at different scan rates.

Scan rate/ mV s^{-1}	E_{pa}/V	E_{pc}/V	I_{pa}/ µA	I_{pc}/ µA	ΔE_p / V	I_{pa} / I_{pc}
25	0.233	0.174	2.900	2.910	0.059	0.997
50	0.232	0.174	4.600	4.550	0.058	1.011
75	0.239	0.176	6.880	6.720	0.063	1.024
100	0.238	0.180	7.380	7.580	0.058	0.974
250	0.238	0.178	11.730	11.590	0.060	1.012
500	0.240	0.175	16.500	15.900	0.065	1.038

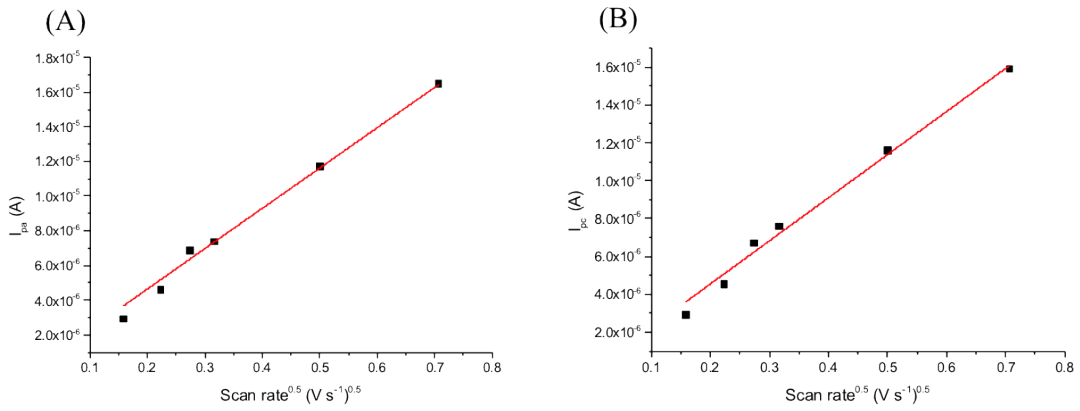

Fig. S4-3. Plots of (A) I_{pa} and (B) I_{pc} against (scan rate)$^{1/2}$ for macrocycle **7a**.

Macrocycle **7a** exhibits a quasi-reversible Fc/Fc^+ redox couple.

[2]Rotaxane **1a**

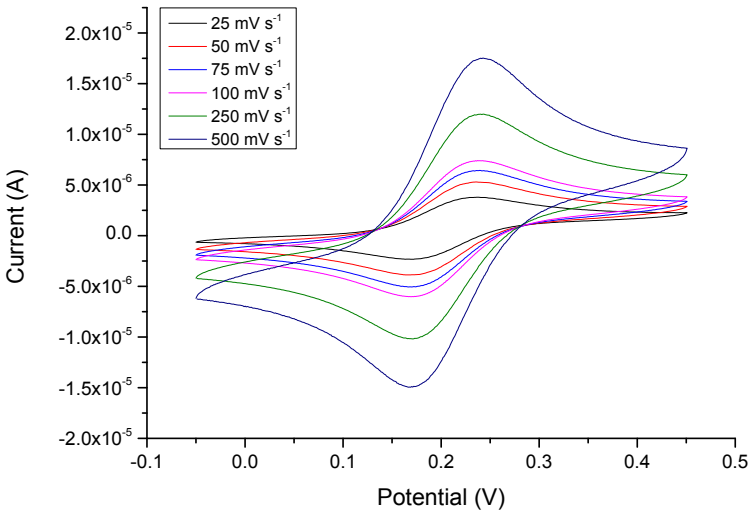

Fig. S4-4. CVs of [2]rotaxane **1a** at different scan rates.

Table S4-2. Values of E_{pc}, E_{pa}, ΔE_p and I_{pa}/ I_{pc} for [2]rotaxane **1a** at different scan rates.

Scan rate/ mV s^{-1}	E_{pa}/V	E_{pc}/V	I_{pa}/ μA	I_{pc}/ μA	ΔE_p / V	I_{pa} / I_{pc}
25	0.232	0.172	3.080	3.040	0.060	1.013
50	0.232	0.171	4.570	4.460	0.061	1.025
75	0.233	0.174	5.540	5.420	0.059	1.022
100	0.235	0.172	6.720	6.240	0.063	1.077
250	0.234	0.172	10.900	10.400	0.062	1.048
500	0.236	0.174	16.800	15.900	0.062	1.057

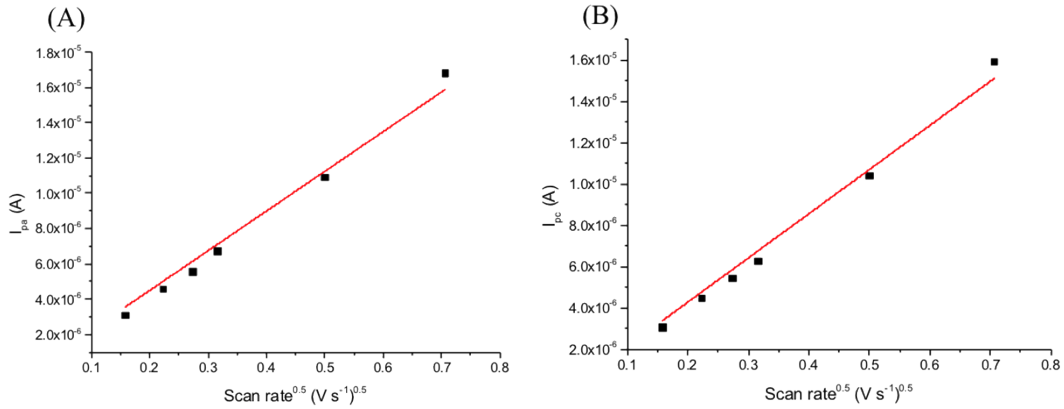

Fig. S4-5. Plots of (A) I_{pa} and (B) I_{pc} against $(\text{scan rate})^{1/2}$ for [2]rotaxane **1a**.

[2]Rotaxane **1a** exhibits a quasi-reversible Fc/Fc^+ redox couple.

[2]Rotaxane **1b**

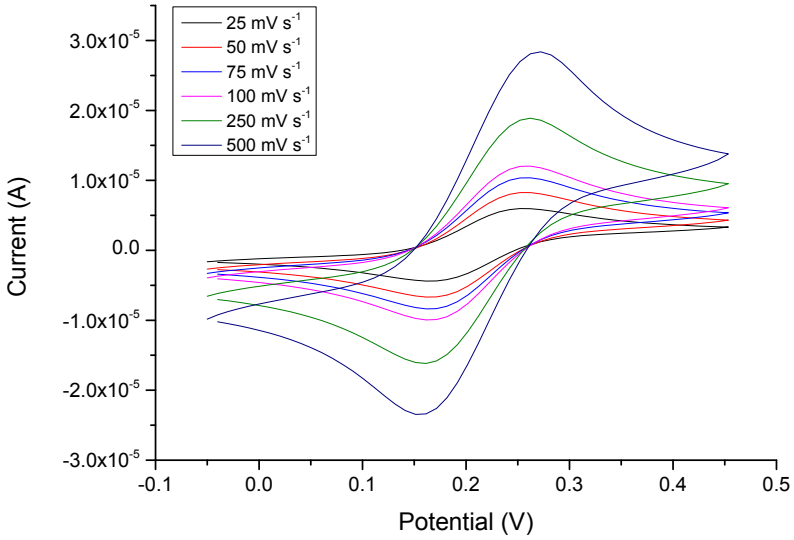

Fig. S4-6. CVs of [2]rotaxane **1b** at different scan rates.

Table S4-3. Values of E_{pc}, E_{pa}, ΔE_p and I_{pa}/ I_{pc} for [2]rotaxane **1b** at different scan rates.

Scan rate/ mV s^{-1}	E_{pa}/V	E_{pc}/V	I_{pa}/ µA	I_{pc}/ µA	ΔE_p / V	I_{pa} / I_{pc}
25	0.252	0.172	4.569	4.635	0.080	0.986
50	0.252	0.172	6.589	6.643	0.080	0.992
75	0.252	0.172	8.258	8.309	0.080	0.994
100	0.252	0.172	9.671	9.712	0.080	0.996
250	0.262	0.161	15.140	15.270	0.101	0.991
500	0.272	0.161	22.440	21.750	0.111	1.032

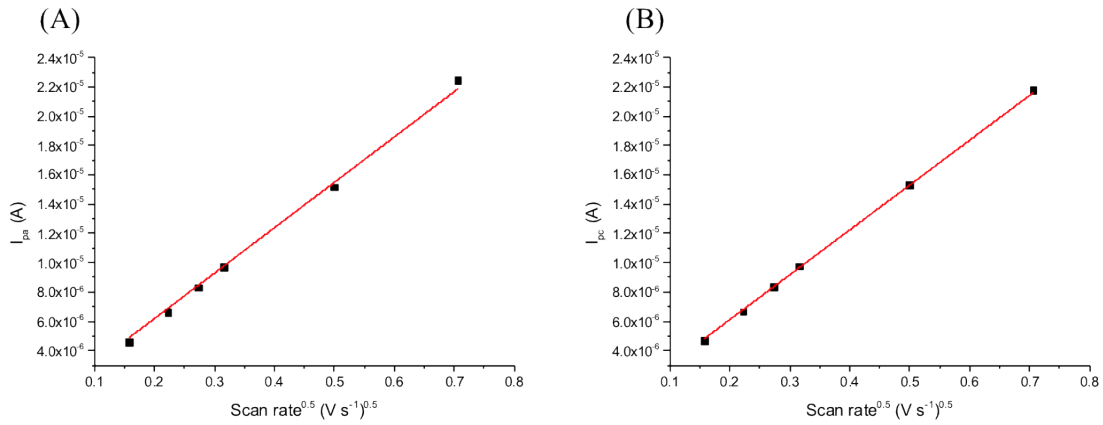

Fig. S4-7. Plots of (A) I_{pa} and (B) I_{pc} against (scan rate)$^{1/2}$ for [2]rotaxane **1b**.

[2]rotaxane **1b** exhibits a quasi-reversible Fc/Fc^+ redox couple.

[2]Rotaxane **1c**

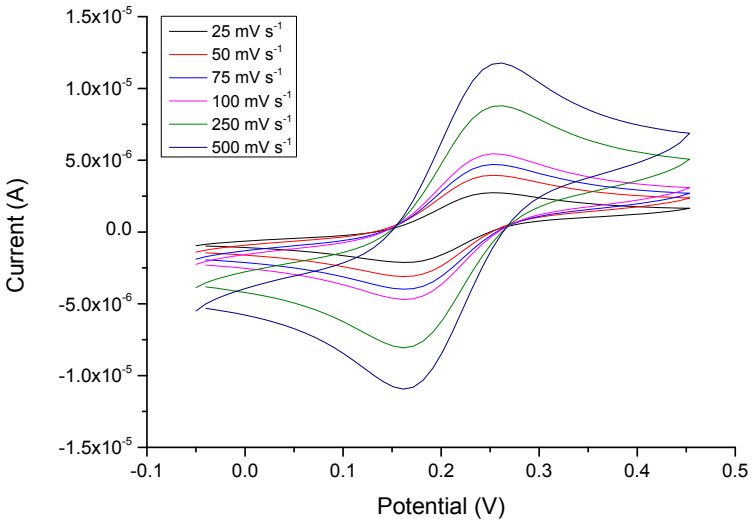

Fig. S4-8. CVs of [2]rotaxane **1c** at different scan rates.

Table S4-4. Values of E_{pc}, E_{pa}, ΔE_p and I_{pa}/ I_{pc} for [2]rotaxane **1c** at different scan rates.

Scan rate/ mV s^{-1}	E_{pa}/V	E_{pc}/V	I_{pa}/ μA	I_{pc}/ μA	ΔE_p / V	I_{pa} / I_{pc}
25	0.252	0.172	2.042	2.078	0.080	0.983
50	0.252	0.172	2.954	2.971	0.080	0.994
75	0.252	0.172	3.645	3.654	0.080	0.998
100	0.252	0.172	4.257	4.263	0.080	0.999
250	0.252	0.172	6.840	7.183	0.080	0.952
500	0.252	0.172	9.272	9.759	0.080	0.950

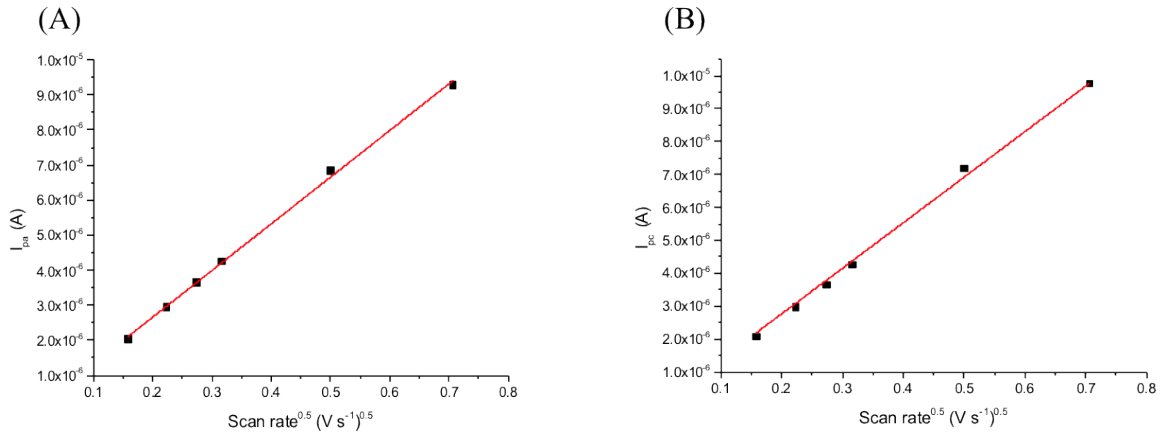

Fig. S4-9. Plots of (A) I_{pa} and (B) I_{pc} against $(\text{scan rate})^{1/2}$ for [2]rotaxane **1c**.

[2]rotaxane **1c** exhibits a quasi-reversible Fc/Fc^+ redox couple.

[2]Rotaxane **1d**

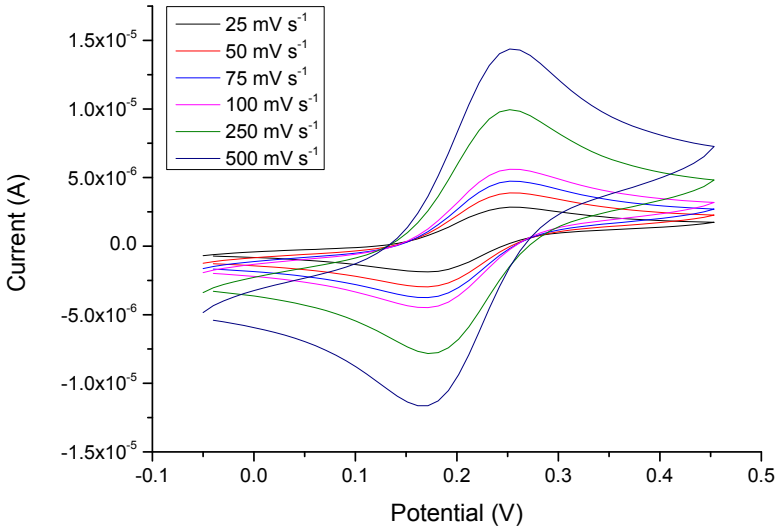

Fig. S4-10. CVs of [2]rotaxane **1d** at different scan rates.

Table S4-5. Values of E_{pc}, E_{pa}, ΔE_p and I_{pa}/ I_{pc} for [2]rotaxane **1d** at different scan rates.

Scan rate/ mV s^{-1}	E_{pa}/V	E_{pc}/V	I_{pa}/ μA	I_{pc}/ μA	ΔE_p / V	I_{pa}/ I_{pc}
25	0.252	0.182	2.018	2.024	0.070	0.997
50	0.252	0.182	2.904	2.950	0.070	0.984
75	0.252	0.182	3.603	3.648	0.070	0.988
100	0.252	0.182	4.270	4.320	0.070	0.988
250	0.252	0.182	7.890	7.413	0.070	1.064
500	0.252	0.172	11.210	10.480	0.080	1.070

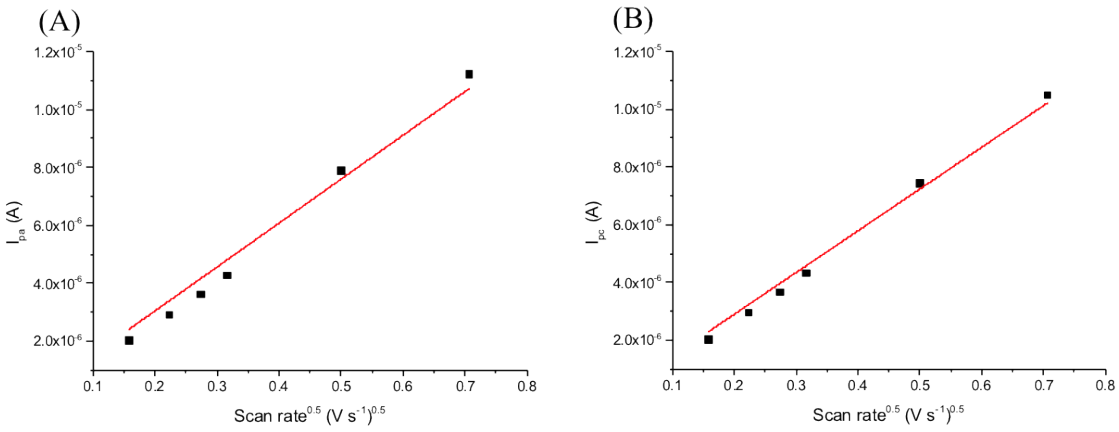

Fig. S4-11. Plots of (A) I_{pa} and (B) I_{pc} against $(\text{scan rate})^{1/2}$ for [2]rotaxane **1d**.

[2]rotaxane **1d** exhibits a quasi-reversible Fc/Fc^+ redox couple.

[2]Rotaxane **1e**

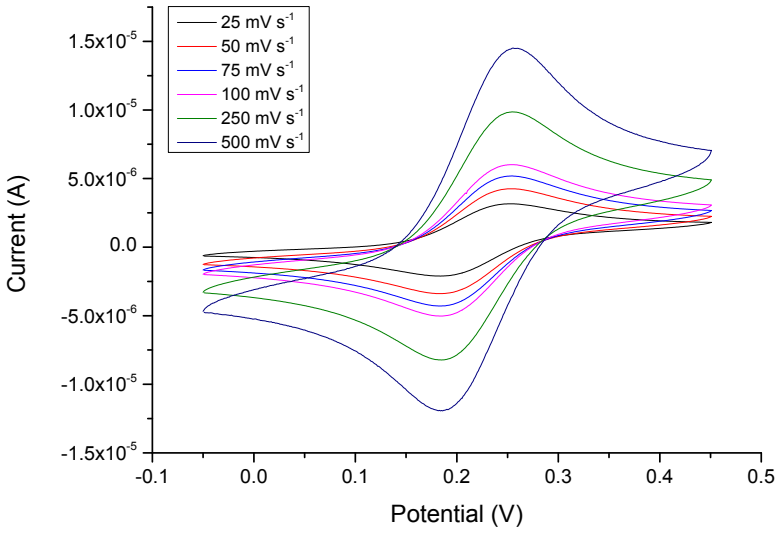

Fig. S4-12. CVs of [2]rotaxane **1e** at different scan rates.

Table S4-6. Values of E_{pc}, E_{pa}, ΔE_p and I_{pa}/ I_{pc} for [2]rotaxane **1e** at different scan rates.

Scan rate/ mV s^{-1}	E_{pa}/V	E_{pc}/V	I_{pa}/ µA	I_{pc}/ µA	ΔE_p / V	I_{pa}/ I_{pc}
25	0.253	0.184	1.446	1.569	0.069	0.922
50	0.255	0.185	3.445	3.595	0.070	0.958
75	0.254	0.182	4.375	4.442	0.072	0.985
100	0.254	0.183	4.999	5.164	0.071	0.968
250	0.254	0.185	8.249	8.364	0.069	0.986
500	0.255	0.186	12.120	12.100	0.069	1.002

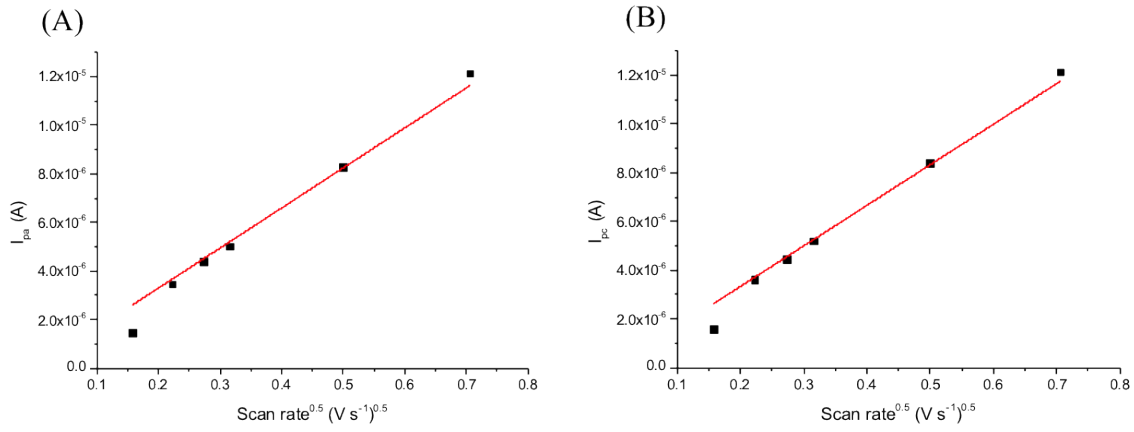

Fig. S4-13. Plots of (A) I_{pa} and (B) I_{pc} against (scan rate)$^{1/2}$ for [2]rotaxane **1e**.

[2]rotaxane **1e** exhibits a quasi-reversible Fc/Fc^+ redox couple.

Data for Electrochemical Anion titrations

Macrocycle **7a**

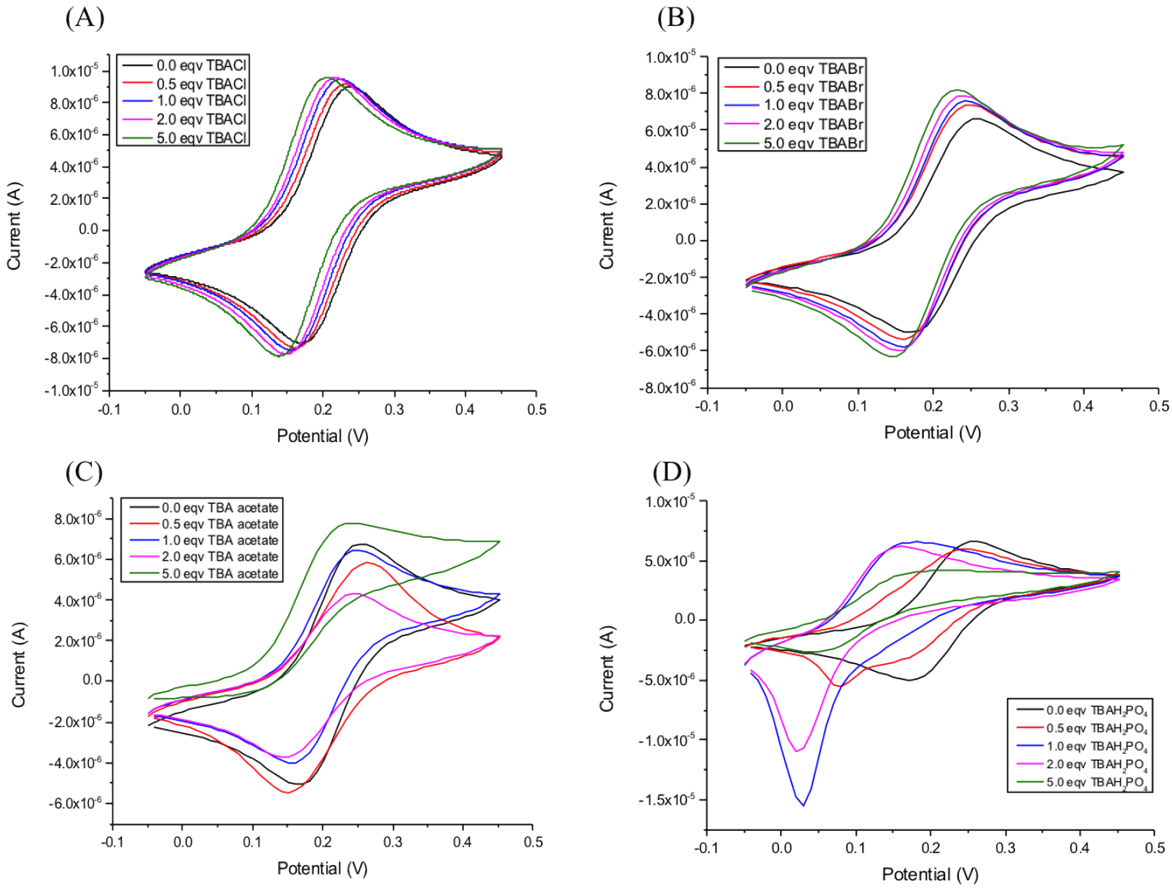

Fig. S4-14. CVs of macrocycle **7a** upon the addition of 0.0, 0.5, 1.0, 2.0 and 5.0 equivalents of (A) TBACl; (B) TBABr; (C) TBA acetate and (D) $TBAH_2PO_4$. TBA acetate was used instead of TBAI due to the fact that oxidation of iodide fell within the electrochemical window of interest.

Chloride Binding Studies for [2]Rotaxane **1b-e**

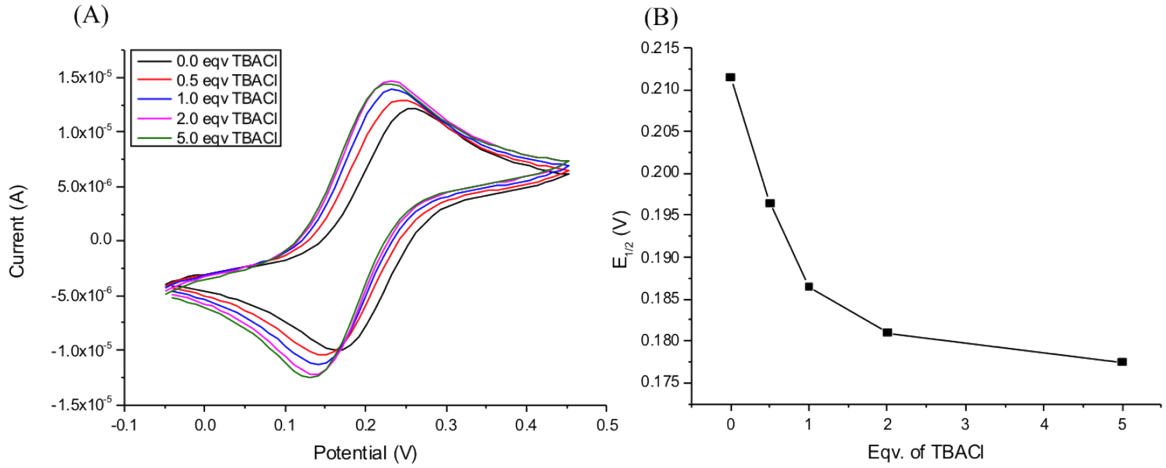

Fig. S4-15. (A) CVs of [2]rotaxane **1b** upon the addition of 0.0, 0.5, 1.0, 2.0 and 5.0 equivalents of TBACl. (B) Plot of $E_{1/2}$ against equivalents of chloride anion added for [2]rotaxane **1b**.

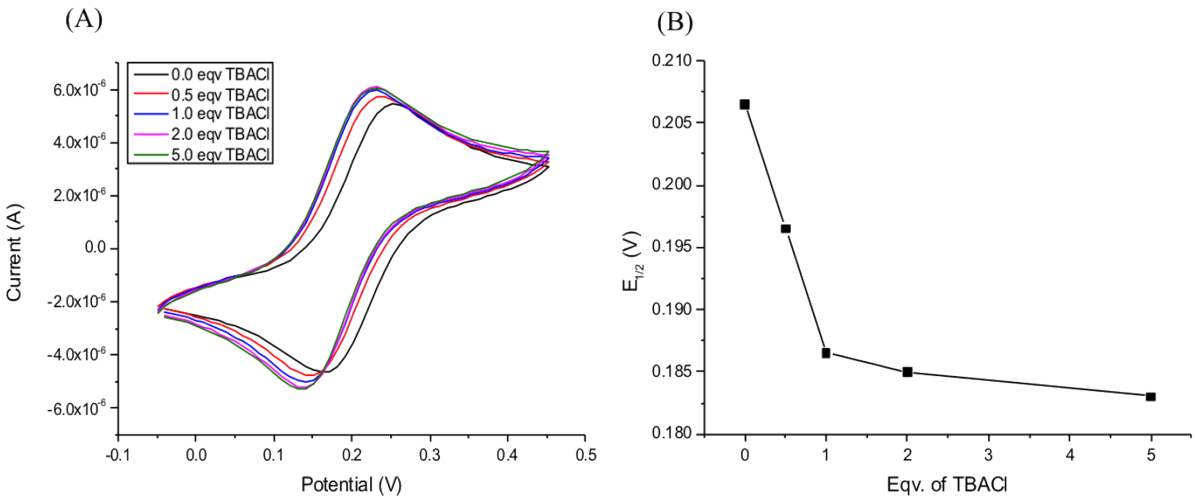

Fig. S4-16. (A) CVs of [2]rotaxane **1c** upon the addition of 0.0, 0.5, 1.0, 2.0 and 5.0 equivalents of TBACl. (B) Plot of $E_{1/2}$ against equivalents of chloride anion added for [2]rotaxane **1c**.

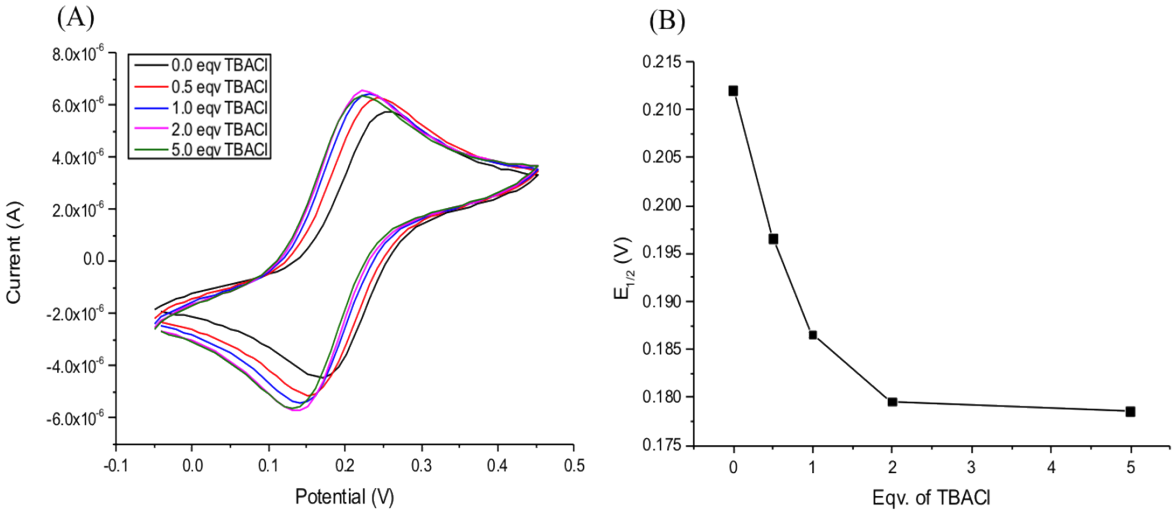

Fig. S4-17. (A) CVs of [2]rotaxane **1d** upon the addition of 0.0, 0.5, 1.0, 2.0 and 5.0 equivalents of TBACl. (B) Plot of $E_{1/2}$ against equivalents of chloride anion added for [2]rotaxane **1d**.

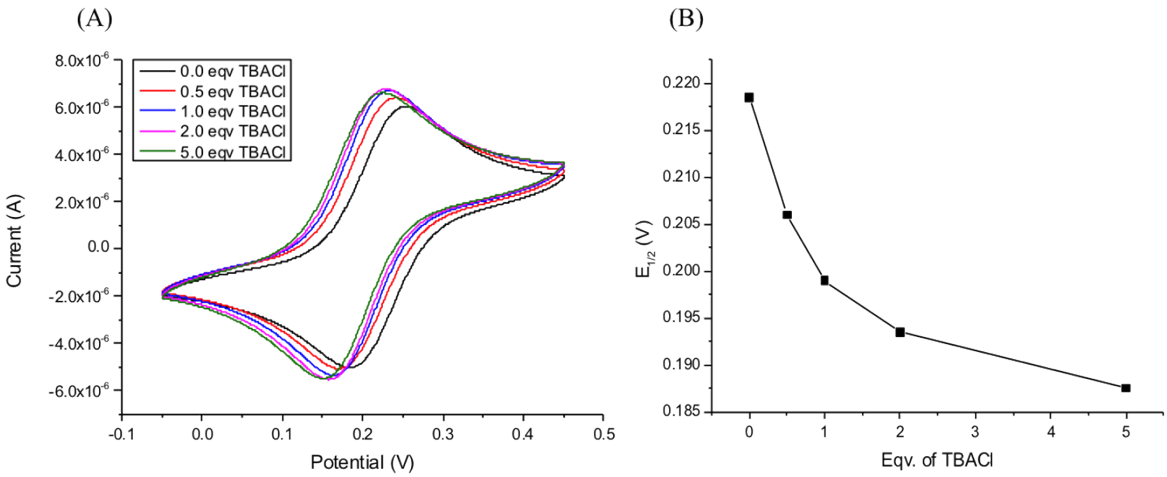

Fig. S4-18. (A) CVs of [2]rotaxane **1e** upon the addition of 0.0, 0.5, 1.0, 2.0 and 5.0 equivalents of TBACl. (B) Plot of $E_{1/2}$ against equivalents of chloride anion added for [2]rotaxane **1e**.

References

1. M. J. Hynes, *J. Chem. Soc. Dalton Trans.*, 1993, 311-312.
2. B. Kratochvil, E. Lorah and C. Garber, *Anal. Chem.*, 1969, **41**, 1793-1796.